SYNTHESIS AND PHOTO-CATALYTIC STUDIES OF ZnS NANOPARTICLES

Thesis submitted as a partial fulfillment for award of the degree of

Masters of Science

in

Physics

Submitted by

Jagdeep Kaur

M. Sc. 2nd Yr (Physics)

(300804010)

Under the guidance

of

Dr. O. P. Pandey

Professor and Head

School of Physics and Materials Science

THAPAR UNIVERSITY

PATIALA

CERTIFICATE

This is to certify that Miss *Jagdeep Kaur*, Roll No. 300804010 has worked on this thesis report as a final fulfillment for award of the degree of *MASTERS OF SCIENCE* in Physics. I certify that the matter embodied in this report is of the candidate's own record and not submitted to any other university in any part or full form for the award of such kind of a degree.

Dr. O. P. Pandey
Supervisor
&
Head
School of Physics and Materials Science
Thapar University
Patiala

Dr. R. K. Sharma 23/7/10
Dean of Academic Affairs
Thapar University
Patiala

2

ACKNOWLEDGEMENT

No matter how much enterprising and entrepreneurial one's thinking is, yet nobody can do everything all by himself without some help and guidance. It is inhumane if the concerned person's assistance goes without appreciation and thanks. My first and foremost offering of thanks goes to the architect who shaped my dreams into reality, my guide and mentor O. P. Pandey, Prof. and Head, School of Physics and Material Science, Thapar University, Patiala. Perseverance, exuberance, positive approaches are just some of the traits he imprinted on my personality. He steered me this journey through his invaluable advice, positive criticism, stimulating discussion and consistent encouragement. His meticulous attention towards my proceedings, his devoted time and his ideas has enabled me to make the project a success. His faith in me has always made me more confident. It had been my privilege to work under his guidance.

My greatest thanks is to research scholar Manoj Sharma for any kind of help and valuable suggestions whenever I needed out of his busy schedule. He has been very helpful in improving dissertation. I am grateful to him for sharing his time and expertise. His comments and views were very insightful and helpful.

My special thanks to Mr. Purushottam Singh who helped me a lot for characterizing the synthesized samples.

I am very thankful to chemistry department specially Prof. Susheel Mittal, Phd. Scholar, Dincsh sir for allowing to use their instruments.

All the faculties and my colleagues of School of Physics and Material Science especially Paramjyot Kumar Jha and my friend Neeraj Mittal are acknowledged for providing me a friendly atmosphere and encouraging me throughout this work.

Last but not the least, I would like to thank my parents for their moral support that kept my spirit up during the endeavor.

Jagdeep Kaur

Jagdeep Kaur

CONTENTS

ABSTRACT

In this work, we report on the synthesis of ZnS semiconductor nanoparticles stabilized with different capping agents (SPP, STTP, SHMP, ME, TG). The capped ZnS nanoparticles were synthesized by a chemical route. The as obtained nanoparticles were characterized by X-ray diffraction (XRD), scanning electron microscopy (SEM), energy dispersive analysis (EDAX), UV–VIS absorption, and photoluminescence (PL) spectra. X-ray diffraction (XRD) study confirmed the formation of wurtzite FCC structure of capped ZnS nanoparticles. Scanning electron microscopic image as well as XRD studies confirmed the nanometer size particles formation. The average particle size was found to lie in the range of 2-8 nm. A UV-VIS optical spectroscopy study was carried out to determine the band gap of the capped ZnS nanoparticles and it showed a blue shift with respect to the bulk value. The room temperature photoluminescence spectra of the nanoparticles showed emission peaks in the range of 363 – 446 nm at excitation wavelength of 325 nm for different concentrations of capping agents in ZnS nanoparticles. Photocatalytic degradation of bromophenol blue dye was done using capped ZnS nanoparticles. It took about 3.5 hours to degrade the dye completely under UV irradiation.

CHAPTER - 1

Introduction

1.1 Definition:

Nano is a Greek word derived from nanos-meaning “dwarf”. This prefix is used in the matric system to mean 10^{-9} or one billionth. Thus a nanometer is 10^{-9} or one billionth of a meter. In comparison, a DNA double-helix has a diameter around 2 nm, typical carbon-carbon bond lengths, or the spacing between these atoms in a molecule are in the range 0.12–0.15 nm, the smallest cellular life-forms, the bacteria of the genus Mycroplasma, are around 200 nm in length and the comparative size of a nanometer to a meter is the same as that of a marble to the size of the earth [1] .There are two terms related to nano and these are nanoscience and nanotechnology. Nanoscience is the study of phenomena and manipulation of materials at the atomic, molecular and macromolecular scales where properties differ significantly from those at a larger scale**.**The design, characterization, production and application of structures, devices and systems by controlled manipulation of size and shape at the nanoscale (atomic, molecular or macromolecular scale) that produces structures devices and systems with at least one novel/superior characteristic or property. 'Nanotechnology' is the engineering of functional systems at the molecular scale. This covers current work and concepts that are more advanced. In its original sense, nanotechnology refers to the projected ability to construct items from the bottom up, using techniques and tools being developed today to make complete, highly advanced products [2].

1.2 Why we study nano:

One obvious question is that why we are interested in nano only? The answers to these questions are that changes in various properties of materials occur at nanoscale. Let us take the example of gold. As shown in figure 1.2, gold in bulk state is always gold in colour and inert but when we study gold at nanoscale, its physical and chemical properties change.

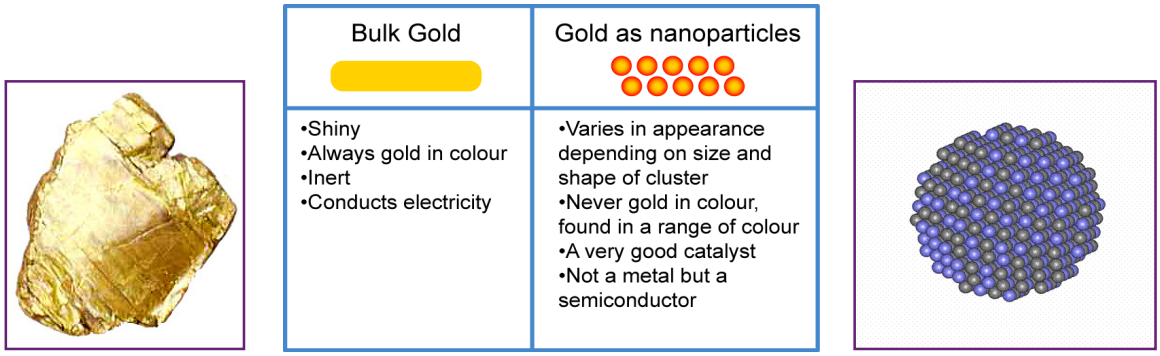

Fig.1.2 – Comparison of bulk gold and gold at nanoscale

1.3 Variation in properties of nanomaterials:

1.3(a) Dominance of electromagnetic forces:

As shown in Fig. 1.3(a), gravitational force is a function of mass and distance. This force becomes weak between nanosized particles as mass of nanosized particles is very less as compared to the particles in bulk. Electromagnetic force is a function of charge and distance and is not affected by mass, so it can be very strong even when we have nanosized particles. The electromagnetic force between two protons is 10^{36} times stronger than the gravitational force.

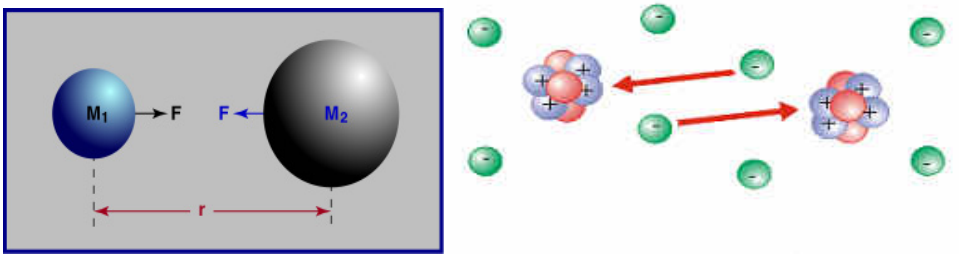

Fig. 1.3(a) – Demonstration of electromagnetic forces

1.3(b) Quantum confinement:

The quantum confinement effect can be observed once the diameter of the particle is of the magnitude of the wavelength of electron wave function. When the materials are so small, their electronic and optical properties deviate substantially from those of bulk materials. A particle

behaves as if it were free when the confining dimension is large compared to the wavelength of the particle. During this state, band gap remains at its original energy due to continuous energy state. However, as the confining dimension decreases and reaches a certain limit, typically in nanoscale, the energy spectrum turns to discrete. As a result, band-gap becomes size dependent. This ultimately results a blue shift in optical illumination as the size of the particles decreases. Specifically, the effect describes the phenomenon that results from electrons and holes being squeezed into a dimension which approaches a critical quantum measurement, called the exciton Bohr radius. A quantum dot confines in all three dimensions such as a small sphere, a quantum wire confines in two dimensions, and a quantum well confines in one dimension [3].

1.3(c) Surface area to volume ratio:

As shown in the Fig.1.3(c) when we cut a cube into smaller and smaller pieces, surface area increases. As a result surface area to volume ratio increases and greater amount of a substance comes in contact with surrounding material. This results in better catalysts, since a greater proportion of the material is exposed for potential reaction [4].

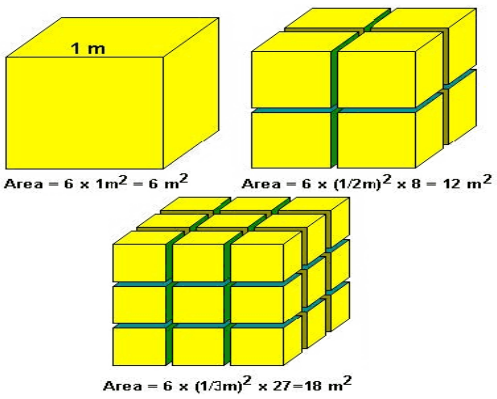

Fig. 1.3(c) – Variation of surface area with decreasing dimensions

1.3(d) Brownian motion:

Brownian motion is the erratic and constant movement of tiny particles when they are suspended in a fluid or gas (Fig. 1.3(d)). For example, if we sprinkle tiny grains of dust into some water, and then look at the dust particles under a microscope, the dust particles will appear to dance around, quite randomly. The phenomenon was discovered by the British botanist Robert

Brown. Further experiments by Brown and others showed that the motion became more rapid and the particles moved farther in a given time interval when the temperature of the water was raised, when the viscosity of the fluid was lowered, or when the size of the particles was reduced [5]. We can conclude that lighter the particles faster the motion and denser the particles slower the motion [6]. Hence Brownian motion is very fast in case of nanomaterials.

Fig. 1.3(d) – Brownian motion of particle

1.3(e) Optical properties (color, transparency):

As particle size decreases, electromagnetic radiation interacts with free electrons to absorb, reflect or transmit different colors of light. With change in particle size band gap of semiconductor changes and corresponding emission color changes (Fig. 1.3(e))

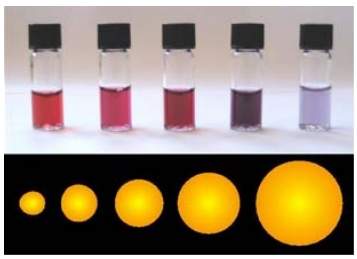

Fig.1.3(e) – Change in emission wavelength with decreasing size

1.3(f) Electrical properties (conductivity):

As shown in the Fig. 1.3(f), band energy increases when the particle size is decreased. We know that if band energy is increased, the conductivity of a material decreases. That's why nanoparticles have decreased conductivity.

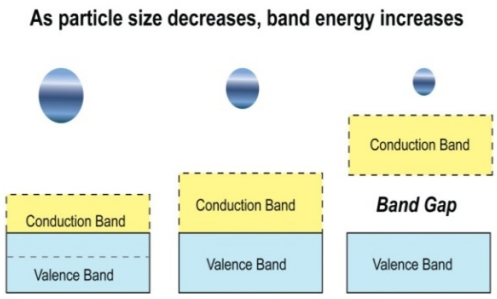

Fig. 1.3(f) – Variation of band-gap with decrease in particle size

1.3(g) Physical properties (hardness, melting point):

Temperature at which the atoms, ions, or molecules in a substance have enough energy to overcome the intermolecular forces that hold them in a "fixed" position in a solid is called its melting point**.** Surface atoms require less energy to move because they are in contact with fewer atoms of the substance**.** Hence we can conclude that nanomaterials have less melting point as compared to their bulk value.

1.3(h) Chemical properties (reactivity, reaction rates):

When particle size is reduced to nanoscale, the ratio of surface area to volume increases dramatically. Since many important chemical reactions including those involving catalysts, occur at surfaces, it is not too surprising that very small particles are staggeringly reactive. This is one of the reasons that chemists are very excited about nanoscience – if they can make more surface area, they get more catalytic action, giving the potential to speed up almost all physical and manufacturing processes.

1.4 Some interesting facts:

As we have discussed earlier that materials reduced to nanoscale can show different properties compared to what they exhibit on macroscale, enabling unique applications. For instance, opaque substances become transparent (copper); stable materials turn combustible (aluminium); solids turn into liquids at room temperature (gold); insulators become conductors (silicon). A material such as gold, which is chemically inert at normal scales, can serve as a potent chemical catalyst at nanoscale. Much of the fascination with nanotechnology stems from these quantum and surface phenomenon that is exhibited by matter at nanoscale**.**

1.5 History of nano:

Although the term nanotechnology got its definition in 1974, the actual concept was introduced way back in 1867, when James Clerk Maxwell proposed a minuscule entity called Maxwell's Demon that was capable of handling individual molecules. Richard Adolf Zsigmondy was the first person to observe and measure the dimensions of nanoparticles. He was also the first person to use nanometer for characterizing the size of the nanoparticles unambiguously. He determined that 1 nm was 1/1,000,000 millimeter. He also developed the first classification system that was based on size of the particle that ranged in nanometer. In the 20th century several developments took place that helped in characterizing nanomaterials. Like in 1920, Irving Langmuir introduced the concept of monolayer, where a layer of material is just one molecule thick. He received a Nobel Prize for this concept. The first use of the concepts found in 'nano-technology' (but pre-dating use of that name) was in "There's Plenty of Room at the Bottom" a talk given by physicist Richard Feynman at an American Physical Society meeting at Caltech on December 29, 1959. Feynman described a process by which the ability to manipulate individual atoms and molecules might be developed, using one set of precise tools to build and operate another proportionally smaller set, and so on down to the needed scale. The term "nanotechnology" was defined by Tokyo Science University Professor Norio Taniguchi in a 1974 paper as follows: "'Nano-technology' mainly consists of the processing of, separation, consolidation, and deformation of materials by one atom or by one molecule." In the 1980s the basic idea of this definition was explored in much more depth by Dr. K. Eric Drexler, who promoted the technological significance of nano-scale phenomena and devices through speeches and the books "Engines of Creation: The Coming Era of Nanotechnology" (1986) and "Nanosystems: Molecular machinery, Manufacturing, and Computation", and so the term acquired its current sense. Engines of Creation: The Coming Era of Nanotechnology is considered the first book on the topic of nanotechnology. Nanotechnology and nanoscience got started in the early 1980s with two major developments; the birth of cluster science and the invention of the scanning tunneling microscope (STM). This development led to the discovery of fullerenes in 1985 and carbon nanotubes a few years later. In another development, the synthesis and properties of semiconductor nanocrystals was studied; this led to a fast increasing number of metal and metal oxide nanoparticles and quantum dots [3].

1.6 Types of nanomaterials:

Based on the number of dimensions at nanoscale, nanomaterials are classified into three categories:-

Nanoparticles: they have all the three dimensions at nanoscale.

Nanofilms: they have two dimensions at nanoscale.

Nanorods: they have only one dimension at nanoscale.

1.7 Applications of nanotechnology:

There are many applications of nanotechnology in various fields like sunscreen, cosmetics, food products, packaging industries, surface coatings, electronic circuits and environment cleaning. Below is the detailed discussion of the various applications of nanotechnology in various fields:

Sunscreen and cosmetics: Nano-sized titanium dioxide and zinc oxide are currently used in some sunscreens, as they absorb and reflect ultraviolet (UV) rays and yet are transparent to visible light and so are more appealing to the consumer. Nano-sized iron oxide is used in some lipsticks as a pigment. However, the use of nano particles in cosmetics has raised a number of concerns about consumer safety.

Clays: Clays containing naturally occurring nano particles are widely used as construction materials and are undergoing continuous improvements. Clay particle-based composites containing plastics and nano-sized flakes of clay are also becoming popular in applications such as manufacturing of car bumpers.

Coatings and surfaces: Coatings with thickness controlled at the nano or atomic scale have been in routine production. Recently developed applications include the self-cleaning window, which is coated in highly activated titanium dioxide, engineered to be highly hydrophobic (water repellent) and antibacterial, and coatings based on nano particulate oxides that destroy chemical agents. Wear and scratch-resistant hard coatings are significantly improved by nano scale intermediate layers.

Photocatalytic degradation of dye: Semiconductor nanoparticles such as ZnO and ZnS are used in breaking the dye using ultraviolet rays. This application is described in detail in section 2.

Textiles: A range of enhanced textiles, such as breathable, waterproof and stain-resistant fabrics are also being developed with the help of nanotechnology. The dust and stain may not retain in the fabric as the pore sizes of these nano materials are smaller than the dust and stain particles.

Tougher and harder cutting tools: Cutting tools made of nano crystalline materials, such as tungsten carbide, tantalum carbide and titanium carbide, are more wear and erosion-resistant, and last longer than their conventional (customary) large-grained counterparts. They are finding applications in the drills used to bore holes in circuit boards. These cutting tools are tougher and harder than the conventional ones.

Paints: Incorporating nano particles in paints could improve their performance, for example, by making them lighter and giving them different properties. Thinner paint coatings ('light weighting'), used for example on aircraft, would reduce their weight and could be beneficial to the environment. Nano paints are brighter and durable than conventional paints. Other novel, and more long-term, application of nano paint is producing paints which can change colour in response to change in temperature or chemical environment.

Fuel cells: One of the suggested solutions for the future fuel crisis is generating electric energy from fuel cells, especially for vehicles. Hydrogen is used as the immediate fuel in fuel cells, which can be generated from hydrocarbons by catalytic (induced) reforming. The potential use of nano-engineered membranes to intensify catalytic processes could enable higher-efficiency, small-scale fuel cells. One of the major practical concerns with regard to fuel cells is storing hydrogen in a portable manner. Research is being conducted to use nano materials such as fullerenes, as a hydrogen storage media [7].

Nano technology provides solutions to many problems currently faced by the people. As an outcome, it is widely becoming popular throughout the globe. We are certain to see many more applications of nanotechnology in the near future.

1.8 Methods for the synthesis of nanomaterials:

There are two approaches for synthesis of nano materials and the fabrication of nano structures. Top down approach refers to slicing or successive cutting of a bulk material to get nano sized particles. Bottom up approach refers to the buildup of a material from the bottom: atom by atom, molecule by molecule or cluster by cluster. There are advantages and disadvantages in both approaches. The biggest problem with top down approach is the imperfection of surface structure and significant crystallographic damage to the processed patterns. These imperfections lead to extra challenges in the device design and fabrication. But this approach leads to the bulk production of nano material. Regardless of the defects produced by top down approach, they will continue to play an important role in the synthesis of nano structures. Though the bottom up approach oftenly referred in nanotechnology, it is not a newer concept. All the living beings in nature observe growth by this approach only and also it has been in industrial use for over a century. Examples include the production of salt and nitrate in chemical industry. Bottom up approach promises a better chance to obtain nano structures with less defects, more homogeneous chemical composition. On the contrary, top down approach most likely introduces internal stress, in addition to surface defects and contaminations [8].

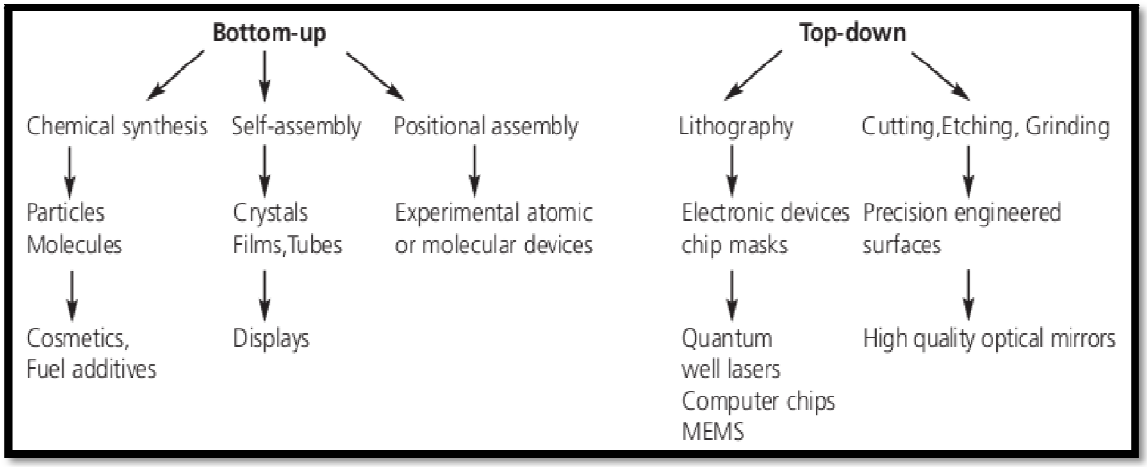

Fig.1.8 – Comparison of bottom up and top down processes

Both the top-down and the bottom-up approaches may be carried out in gas, liquid or solid states, with a variety of different applications. These applications have their interest in controlling particle size, particle shape, size distribution, particle composition and degree of particle

agglomeration. Bottom-up manufacturing involves constructing structures either atom-by-atom or molecule-by-molecule. The different techniques to achieving the goal of bottom-up manufacturing can be split into three categories:

1.) Chemical Synthesis

2.) Self-Assembly

3.) Positional Assembly

1.9 Characterization techniques:

Many techniques are used to identify the various properties of nanomaterials. Some of the most important techniques are discussed below:

1.9(a) X-ray diffraction technique (XRD):

X-ray diffraction (XRD) is a versatile, non-destructive technique that reveals detailed information about the chemical composition and crystallographic structure of natural and manufactured materials. In a crystalline solid, the constituent particles (atoms, ions or molecules) are arranged in a regular order. An interaction of a particular crystalline solid with X-rays helps in investigating its actual structure. Crystals are found to act as diffraction gratings for X-rays and this indicates that the constituent particles in the crystals are arranged in planes at close distances in repeating patterns. The experimental setup is shown in the Fig. 1.9(a).

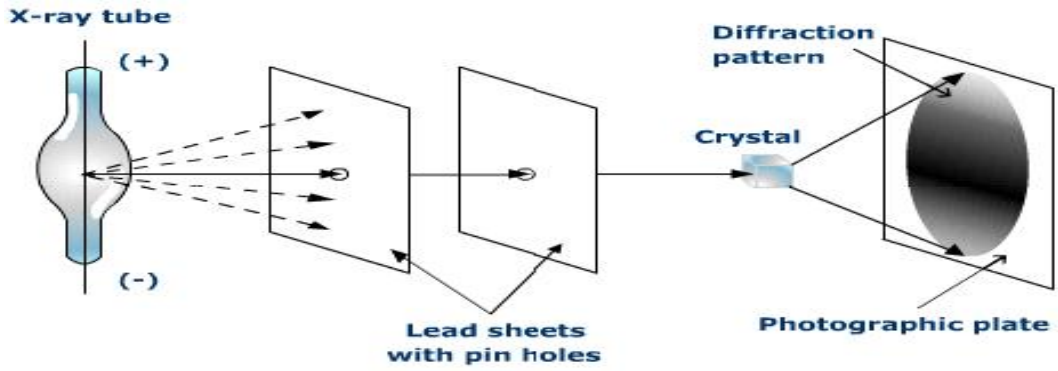

Fig. 1.9(a) – Experimental set-up of XRD

The diffraction patterns were analysed to determine the interplanar distances in a particular crystal. A simple representation of the X-ray diffraction is shown below:

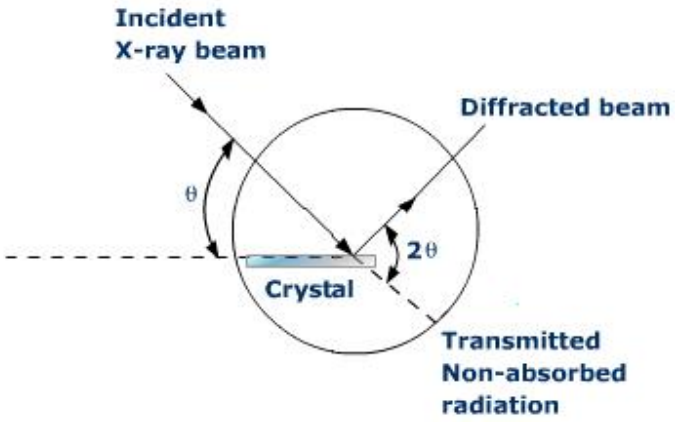

Fig. 1.9(b) - A simple representation of X-ray diffraction

Basic principle:

The process is based upon the principle that a crystal may be considered to be made up of a number of parallel equidistant atomic planes, as represented by lines AB, CD and EF in fig. 1.9(c)

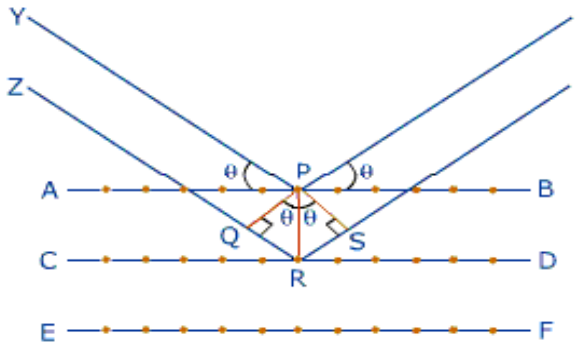

Fig. 1.9(c)

Suppose two waves (Y and Z) of X-ray beams, which are in phase falls on the surface of the crystal. If the ray Y gets reflected from the first layer i.e., AB line and the ray Z is reflected from the second layer of atoms i.e., CD line, then it is evident that as compared to the ray Y, ray Z has

to travel a longer distance, equal to QRS in order to emerge out of the crystal. If the waves Y and Z are in phase after reflection, the difference in distance travelled by the two rays must be equal an integral number of wavelength (nl), for constructive interference [9].

Thus, Distance QRS = nl ..... (i)

It is obvious from the figure that

$$QR = RS = PR \sin q$$

Therefore $QRS = 2\ PR \sin q$ .....(ii)

If the distance between the successive atomic planes is = d

Then, $PR = d$ ...……(iii)

So, from equations (i), (ii) and (iii)

$$nl = 2d \sin q$$

Thus, Bragg gave a mathematical equation to establish a relationship between wave length of the incident X-ray, the distance between the layers and the angle of diffraction.

Here, l = wavelength of x-ray used

q = Angle between incident x-rays and plane of the crystal. The diffracted beam makes an angle 2q.

d = Distance between planes of the constituent particles in a crystal.

n = An integer (1, 2, 3, 4, … etc) which represents the serial order of diffracted beams.

Bragg's equation can be used to calculate the distances between repeating planes of the particles in a crystal. Similarly, if interplanar distances are given, the corresponding wavelengths of the incident beam of X-ray can be calculated.

Scherrer's formula: $t = k\lambda / \beta \cos\theta$

Where t = thickness of crystallite

k = constant dependant on crystallite shape

λ = x-ray wavelength

β = FWHM

θ = bragg angle

When to use Scherrer's formula:

- Crystallite size < 1000 angstrom
- K depends on definition of t and β.
- Within 20-30% accuracy at best.

1.9(b) Scanning Electron Microscope (SEM):

The SEM is a microscope that uses electrons instead of light to form an image. The technique in which SEM is used to characterize the materials is called Scanning Electron Microscopy. Since their development in the early 1950's, scanning electron microscopes have developed new areas of study in the medical and physical science communities. The SEM has allowed researchers to examine a much bigger variety of specimens. The scanning electron microscope has many advantages over traditional microscopes. The SEM has a large depth of field, which allows more of a specimen to be in focus at one time. The SEM also has much higher resolution, so closely spaced specimens can be magnified at much higher levels. Because the SEM uses electromagnets rather than lenses, the researcher has much more control in the degree of magnification. All of these advantages, as well as the actual strikingly clear images, make the scanning electron microscope one of the most useful instruments in research today [10].

Principle and working of SEM:

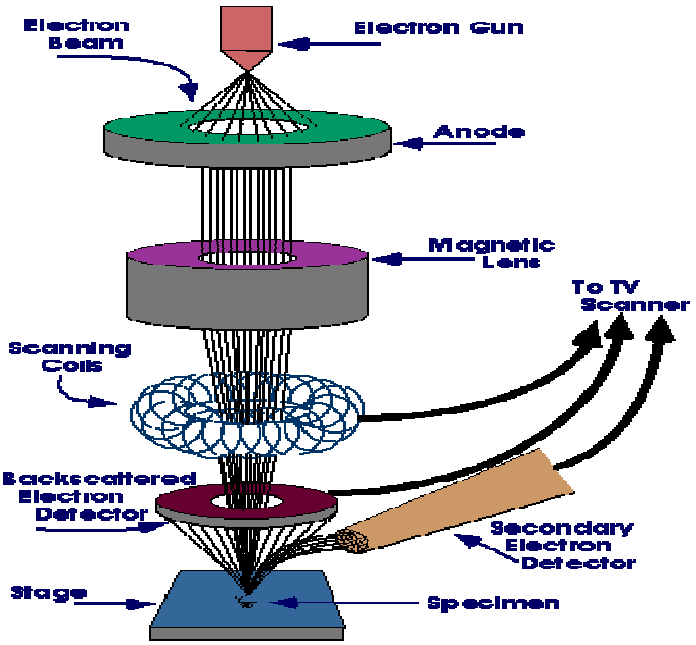

Fig. 1.9(d)

The SEM is an instrument that produces a largely magnified image by using electrons instead of light to form an image. A beam of electrons is produced at the top of the microscope by an electron gun. The electron beam follows a vertical path through the microscope, which is held within a vacuum. The beam travels through electromagnetic fields and lenses, which focus the beam down toward the sample. Once the beam hits the sample, electrons and X-rays are ejected from the sample. Detectors collect these X-rays, backscattered electrons, and secondary electrons and convert them into a signal that is sent to a screen similar to a television screen. This produces the final image.

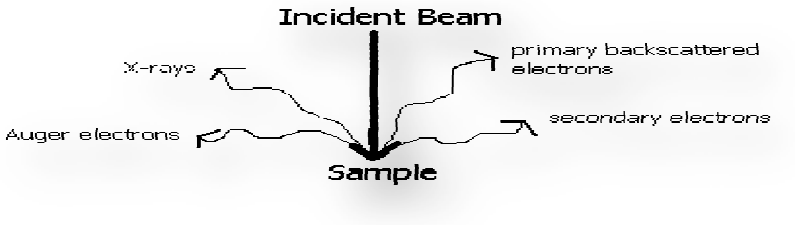

Fig. 1.9(e)

1.9(c) Transmission Electron Microscopy (TEM):

Transmission electron microscopy (TEM) is a microscopic technique whereby a beam of electrons is transmitted through an ultra thin specimen, interacting with the specimen as it passes through. An image is formed from the interaction of the electrons transmitted through the specimen; the image is magnified and focused onto an imaging device, such as a fluorescent screen, on a layer of photographic film.

Working principle:

TEM works like a slide projector. A projector shines a beam of light which transmits through the slide. The patterns painted on the slide only allow certain parts of the light beam to pass through. Thus the transmitted beam replicates the patterns on the slide, forming an enlarged image of the slide when falling on the screen. TEMs work the same way except that they shine a beam of electrons (like the light in a slide projector) through the specimen (like the slide). However, in TEM, the transmission of electron beam is highly dependent on the properties of material being examined. Such properties include density, composition, etc. For example, porous material will allow more electrons to pass through while dense material will allow less. As a result, a specimen with a non-uniform density can be examined by this technique. Whatever part is transmitted is projected onto a phosphor screen for the user to see.

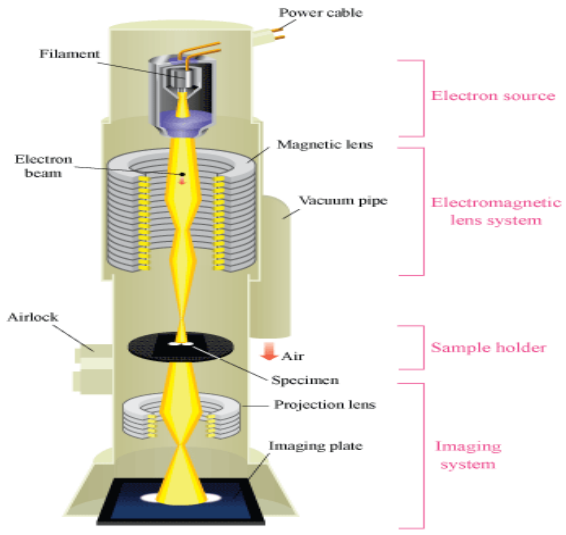

Fig. 1.9(f)

Electron source: The electron source consists of a cathode and an anode. The cathode is a tungsten filament which emits electrons when being heated. A negative cap confines the electrons into a loosely focused beam. The beam is then accelerated towards the specimen by the positive anode. Electrons at the rim of the beam will fall onto the anode while the others at the center will pass through the small hole of the anode. The electron source works like a cathode ray tube.

Electromagnetic lens system: After leaving the electron source, the electron beam is tightly focused using electromagnetic lens and metal apertures. The system only allows electrons within a small energy range to pass through, so the electrons in the electron beam will have a well-defined energy.

Aperture: A thin disk with a small (2-100 micrometers) circular through-hole. It is used to restrict the electron beam and filter out unwanted electrons before hitting the specimen.

Sample Holder: Sample holder is a platform equipped with a mechanical arm for holding the specimen and controlling its position.

Imaging system: The imaging system consists of another electromagnetic lens system and a screen. The electromagnetic lens system contains two lens systems, one for refocusing the electrons after they pass through the specimen, and the other for enlarging the image and projecting it onto the screen. The screen has a phosphorescent plate which glows when being hit by electrons. Image forms in a way similar to photography [11].

1.9(d) UV-VIS spectroscopy:

Ultraviolet-visible spectroscopy or ultraviolet-visible spectrophotometry (UV-VIS or UV/VIS) involves the spectroscopy of photons in the UV-visible region. This means it uses light in the visible and adjacent (near ultraviolet (UV) and near infrared (NIR) ranges. The absorption in the visible ranges directly affects the color of the chemicals involved. In this region of the electromagnetic spectrum, molecules undergo electronic transitions. This technique is complementary to fluorescence spectroscopy, in that fluorescence deals with transitions from the

excited state to the ground state, while absorption measures transitions from the ground state to the excited state [12].

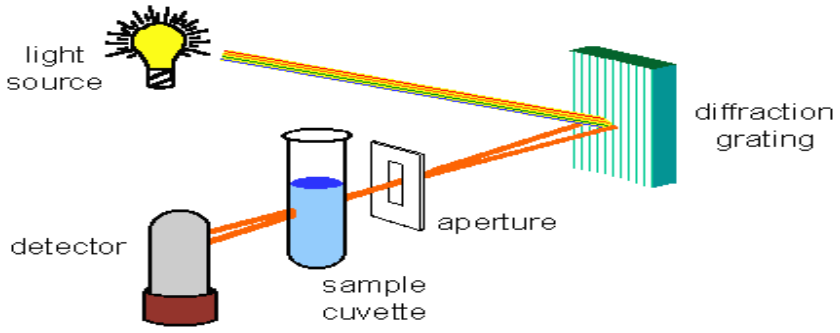

Fig. 1.9(g) - A simple UV-VIS spectrophotometer

The basic parts of a spectrophotometer are a light source, a holder for the sample, a diffraction grating or monochromator to separate the different wavelengths of light, and a detector. The radiation source is often a Tungsten filament (300-2500 nm), a deuterium arc lamp which is continuous over the ultraviolet region (190-400 nm), and more recently light emitting diodes (LED) and Xenon Arc Lamps for the visible wavelengths. The detector is typically a photodiode or a CCD. Photodiodes are used with monochromators, which filter the light so that only light of a single wavelength reaches the detector. Diffraction gratings are used with CCDs, which collects light of different wavelengths on different pixels. UV-Vis spectroscopy is routinely used in the quantitative determination of solutions of transition metal ions and highly conjugated organic compounds.

Basic principle:

Beer-Lambert law: This law states that the absorbance of a solution is directly proportional to the concentration of the absorbing species in the solution and the path length. Thus, for a fixed path length, UV-VIS spectroscopy can be used to determine the concentration of the absorber in a solution. It is necessary to know how quickly the absorbance changes with concentration. The method is most often used in a quantitative way to determine concentrations of an absorbing species in solution, using the Beer-Lambert law:

$$A = -\log_{10}(I/I_0) = \epsilon \cdot c \cdot L$$

Where A is the measured absorbance, I_0 is the intensity of the incident light at a given wavelength, I is the transmitted intensity, L the pathlength through the sample, and c the concentration of the absorbing species. For each species and wavelength, ε is a constant known as the molar absorptivity or extinction coefficient. This constant is a fundamental molecular property in a given solvent, at a particular temperature and pressure, and has units of 1 / M * cm or often AU / M * cm.

Practical considerations:

To actually make a valid measurement we must understand and be aware of the limitations of the particular instrument being used. The molar extinction coefficient, ε, is a function of the wavelength (that is, the color) of the light used. For the Beer-Lambert relation above to hold in a particular case, the light must be sufficiently monochromatic that the exctinction coefficient used is well defined. There can also be limits imposed by the materials being measured [3].

1.9(e) Fourier Transform Infrared Spectroscopy (FTIR):

FTIR is most useful for identifying chemicals that are either organic or inorganic. It can be utilized to quantitate some components of an unknown mixture. It can be applied to the analysis of solids, liquids, and gasses. The term Fourier Transform Infrared Spectroscopy (FTIR) refers to a fairly recent development in the manner in which the data is collected and converted from an interference pattern to a spectrum. Today's FTIR instruments are computerized which makes them faster and more sensitive than the older dispersive instruments.

Physical principles:

Molecular bonds vibrate at various frequencies depending on the elements and the type of bonds. For any given bond, there are several specific frequencies at which it can vibrate. According to quantum mechanics, these frequencies correspond to the ground state (lowest frequency) and several excited states (higher frequencies). One way to cause the frequency of a molecular vibration to increase is to excite the bond by having it absorb light energy. For any given transition between two states the light energy (determined by the wavelength) must exactly equal the difference in the energy between the two states [usually ground state (E_0) and the first excited state (E_1)]. The energy corresponding to these transitions between molecular vibrational states is

generally 1-10 kilocalories/mole which corresponds to the infrared portion of the electromagnetic spectrum.

Difference in energy states = energy of light absorbed

$$E_1 - E_0 = hc / \lambda$$

Where h = plank's constant

c = speed of light

λ = wavelength of light.

Qualitative analysis:

FTIR can be used to identify chemicals from spills, paints, polymers, coatings, drugs, and contaminants. FTIR is perhaps the most powerful tool for identifying types of chemical bonds (functional groups). The wavelength of light absorbed is characteristic of the chemical bond as can be seen in the annotated spectrum. By interpreting the infrared absorption spectrum, the chemical bonds in a molecule can be determined. FTIR spectra of pure compounds are generally so unique that they are like a molecular "fingerprint". While organic compounds have very rich, detailed spectra, inorganic compounds are usually much simpler. For most common materials, the spectrum of an unknown can be identified by comparison to a library of known compounds. We have several infrared spectral libraries including on-line computer libraries. To identify less common materials, IR will need to be combined with nuclear magnetic resonance, mass spectrometry, emission spectroscopy, X-ray diffraction, and/or other techniques [3].

1.9(f) Fluorescence spectroscopy:

Fluorescence spectroscopy, also known as fluorometry or spectrofluorometry, is a type of electromagnetic spectroscopy which analyzes fluorescence from a sample. It involves using a beam of light, usually ultraviolet light, that excites the electrons in molecules of certain compounds and causes them to emit light of a lower energy, typically, but not necessarily, visible light.

Instrumentation:

The light from an excitation source passes through a filter or monochromator, and strikes the sample. A proportion of the incident light is absorbed by the sample and some of the molecules in the sample fluoresce. The fluorescent light is emitted in all directions. Some of this fluorescent light passes through a second filter or monochromator and reaches a detector, which is usually placed at 90° to the incident light beam to minimize the risk of transmitted or reflected incident light reaching the detector.

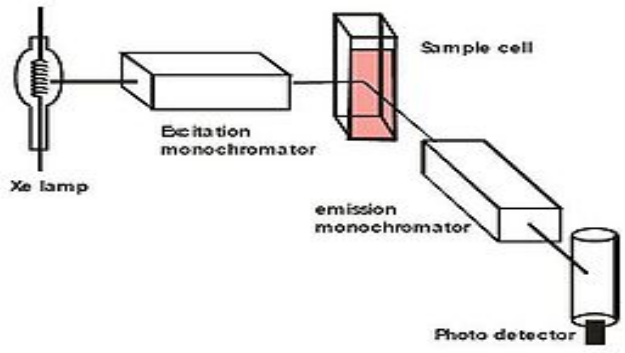

Fig. 1.9(h) – A simple PL spectrophotometer

Theory:

Molecules have various states referred to as energy levels. Fluorescence spectroscopy is primarily concerned with electronic and vibrational states. Generally, the species being examined will have a ground electronic state (a low energy state) of interest, and an excited electronic state of higher energy. Within each of these electronic states are various vibrational states. In fluorescence spectroscopy, the species is first excited, by absorbing a photon, from its ground electronic state to one of the various vibrational states in the excited electronic state. Collisions with other molecules cause the excited molecule to lose vibrational energy until it reaches the lowest vibrational state of the excited electronic state. The molecule then drops down to one of the various vibrational levels of the ground electronic state again, emitting a photon in the process. As molecules may drop down into any of several vibrational levels in the ground state, the emitted photons will have different energies, and thus frequencies. Therefore, by analysing

the different frequencies of light emitted in fluorescent spectroscopy, along with their relative intensities, the structure of the different vibrational levels can be determined. In a typical experiment, the different frequencies of fluorescent light emitted by a sample are measured, holding the excitation light at a constant wavelength. This is called an emission spectrum. An excitation spectrum is measured by recording a number of emission spectra using different wavelengths of excitation light [13].

CHAPTER - 2

Photocatalytic degradation of dye

2.1Introduction:

Different types of dyes are used in many industries such as textile, paint, ink, plastics and cosmetics. The textile industry produces large quantity of highly colored effluents, which are generally toxic and resistant to destruction by biological treatment methods. Therefore, it is necessary to find an effective method to remove color from textile effluents. Other conventional methods of color removal from an aqueous medium include techniques like coagulation, filtration, adsorption by activated carbon and treatment with ozone. These methods are not destructive but only transfer dye from one phase to another. Each method has its own advantages and disadvantages. For example, the use of charcoal is technically easy but has a high waste disposal cost. While in filtration, low-molar-mass dyes can pass through the filter system. Coagulation, using alum, ferric salts or lime is a low cost process. However, the disposal of toxic sludge is a severe drawback in all the above methods. Lastly, the ozone treatment does not require disposal but suffers from high cost [14]. Hence, there is a need for developing treatment technologies for eliminating contaminants from wastewater. Photocatalytic degradation by semiconductors is a new, effective and rapid technique for the removal of pollutants from water. The 2-6 semiconductor photocatalysts have attracted much interest in recent years for their highly active photocatalytic functions, like the ability to decompose chemical compounds, as well as super hydrophilic and antibacterial properties. In photocatalytic processes, a semiconductor photocatalyst is activated with ultraviolet (UV) irradiation. Under illumination, organic molecules react with photogenerated hole or, more probably, with photoinduced hydroxyl radicals, to give a number of hydroxylated reaction intermediates [13, 14]. Various dyes like Congo Red (CR), C.I. Direct Red 80 (DR), C.I. Reactive Red 17 (RR), Methyl Orange (MO), C.I. Direct Yellow 50 (DY), Solophenyl Red 3BL (SR), Coperoxon Navy Blue RL (CN) and Nylosan Black 2-BC.S Acid Black 42 (NB) have been degraded in the presence of UV-light [15].

2.2 Photocatalysis:

Photocatalysis is the acceleration of a photoreaction in the presence of a catalyst. In catalysed photolysis, light is absorbed by an adsorbed substrate. In photogenerated catalysis the photocatalytic activity (PCA) depends on the ability of the catalyst to create electron–hole pairs, which generate free radicals (hydroxyl radicals: ·OH) able to undergo secondary reactions.Catalysts used in such reactions are called photocatalysts, such as chlorophyll in photosynthesis is a natural photocatalyst. Artificial photocatalyst are mainly semiconductor materials [3]. In 1972, Fujishimna and Honda discovered the photocatalytic splitting of water on TiO_2 electrodes [15]. This discovery led to the invention of new field of heterogeneous photocatalysis. The main focus of previous studies have been to investigate the principal applicability of photocatalysis systems for efficient treatment of water polluted with toxic substances and later on quantum size effects on photoreactions for semiconductor nanoparticles have only been extremely studied.

Basic principle and mechanism:

The basic principle behind photocatalysis is relatively simple. Light energy from UV radiation excites electrons on the surface of the photocatalyst, whereby electrons move from the valence band into the conduction band. This leaves positive “holes” in the valence band, which reacts with water leading to the production of radicals that can degrade dyes. (Fig. 2.1)

$$ZnS + h\upsilon \longrightarrow e^- + h^+$$

$$e^- + h^+ \longrightarrow \text{heat}$$

$$h^+ + H_2O_{ads} \longrightarrow \cdot OH + H^+$$

$$h^+ + OH_{ads} \longrightarrow \cdot OH$$

$$h^+ + RH_{ads} \longrightarrow \cdot R + H^+$$

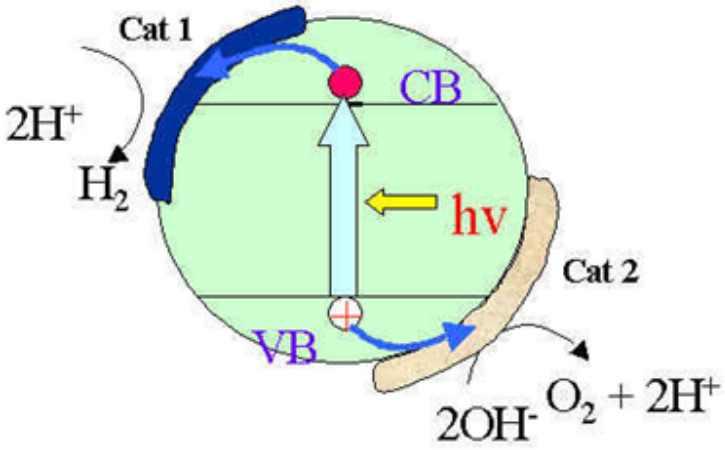

Fig. 2.1 – Mechanism of photocatalysis

The electrons can also react with the compounds that are present in the solution such as oxygen and hydrogen peroxide. The electrons can be absorbed by the oxygen to form superoxide or it can react with oxygen together with hydrogen to create hydrogen peroxide. It can then react with hydrogen peroxide to create hydroxyl radicals and hydroxyl ions.

$$e^- + O_{2ads} \longrightarrow O_2^-$$
$$2e^- + O_{2ads} + 2H^+ \longrightarrow H_2O_2$$
$$e^- + H_2O_{2ads} \longrightarrow {}^{\cdot}OH + OH^-$$

All of these produced species are highly reactive. The electrons when combined with oxygen are stopped from dropping back to the valence band and prevent the electron-hole recombination [16]. This means that the hole and the electron have more time to react with species adsorbed to the catalyst. A lack of dissolved oxygen would hinder the reaction as electron-hole recombination would occur far more readily, giving less time for the species to react.

2.3 Photocatalysts and their activity:

Definition: A substance that is able to produce, by absorption of light quanta, chemical transformations of the reaction participants, repeatedly coming with them into the intermediate chemical interactions and regenerating its chemical composition after each cycle of such

interactions [17]. A requirement for the photo-catalyst is to have a band-gap higher than 2.43 eV, which is the energy needed for the splitting of water.

An ideal photocatalyst should be stable, inexpensive, non-toxic and, of course, highly photoactive. Another primary criteria for the degradation of organic compounds is that the redox potential of the H_2O / $^{\cdot}OH$ couple lies within the band-gap of the semiconductor. Several semiconductors have band-gap energies sufficient for catalysing a wide range of chemical reactions. These include TiO_2, WO_3, $SrTiO_3$, α –Fe_2O_3, ZnO and ZnS [18]. One of the main advantages of the application of the nano-sized particles is the increase in band-gap energy with decreasing particle size. As the size of a semiconductor particle falls below the critical radius, the charge carriers begin to behave quantum mechanically and the charge confinement leads to a series of discrete electronic states. As a result there is an increase in the effective band-gap and a shift of the band edges. Thus by varying the size of semiconductor particles, it is possible to enhance the redox potential [19] of the valence-band holes and the conduction-band electrons.

In brief nanoparticles can be used as photocatalysts due to the following reasons:

1. Their catalytic ability is dependent on the transition of the highest occupied molecular orbital (HOMO) to the lowest unoccupied molecular orbital (LUMO). This transition can be made to occur in the UV and visible light spectrum.
2. Nanoparticles exhibit more efficient turnover rate due to the increase in the catalytic surface area.

CHAPTER – 3

Materials and their use in photocatalysis

3.1 ZnS:

Zinc sulfide or zinc sulphide is a chemical compound with formula ZnS. Zinc sulfide is a white to yellow coloured powder or crystal. It is typically encountered in the more stable cubic form, known as zinc blende or sphalerite. The hexagonal form is known both as a synthetic material and as the mineral wurtzite. Both sphalerite and wurtzite are intrinsic, wide band-gap semiconductors. The cubic form has a band-gap of 3.5 eV at 300K whereas the hexagonal form has a band-gap of 3.91eV.The transition from the sphalerite form to the wurtzite form occurs at around 1020^0C.It can be both doped as n-type semiconductor and p-type semiconductor, which is unusual for the 2-6 semiconductors. ZnS is a covalently bonded solid [3].

Structure of ZnS:

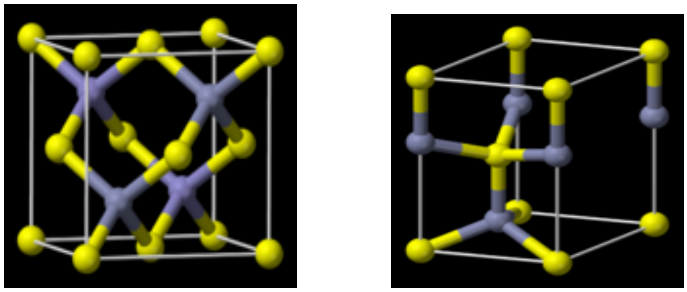

zinc blende Wurtzite

Fig. 3.1 – Two forms of ZnS

3.2 ZnS at nanoscale:

Nanostructured materials have attracted a great deal of attention in the last few years for their unique characteristics that cannot be obtained from conventional macroscopic materials. Owing to quantum size effects and surface effects, nanoparticles can display novel optical, electronic, magnetic, chemical and structural properties that might find many important technological applications. An extremely active and prolific field in nanomaterials is finding ways to control size and morphology of the nanoparticles since the properties and applications of the

nanomaterials are largely dependent on their size and morphology. The most evident manifestation of properties is the optical light emission in the blue-red spectral region characterized by a blue-shift at smaller crystallite dimensions. Such properties make semiconducting nanostructures suitable for several kinds of applications, from anti-reflecting coating to bioelectronics and light-emitting devices. In the past decade, 2-6 semiconductor nanoparticles attract much attention because of their size-dependent (and thus tunable) photo- and electro-luminescence properties and promising applications in optoelectronics. Among the family of 2-6 semiconductors ZnS, CdS, ZnO, CdTe etc. are the foremost candidates because of their favourable optical and electronic properties for optoelectronic applications. Among those, ZnS is a commercially important 2-6 semiconductor having a wide optical gap, rendering it a very attractive material for optical application especially in nanocrystalline form. ZnS can have two different structures (zinc blende and wurtzite), both of which have same band-gap energy (3.68eV) and the direct band structure. ZnS has been used for the cathode-ray tube, the field emission display and the scintillator as one of the most frequently used phosphors. In addition, a ZnS crystal laser has been produced using streamer excitation and thin films of ZnS can be used as an active emitting material in such a device, termed the hot electron cold cathode. Optical and luminescent properties of nanocrystalline ZnS prepared in the forms of thin film, powder and colloid using different synthesis techniques such as sputtering, co-evaporation, wet chemical, sol-gel, solid state, micro-wave irradiation, ultrasonic irradiation or synthesis under high gravity environment were studied in detail. Luminescence measurements were identified as one of the most important techniques to reveal the energy structure and surface states of these particles. Localized trap states inside the band gap were studied in detail to recognize the sub band-gap energy levels. It was observed that the defect levels play an important role in determining the luminescent characteristics of the ZnS nanoparticles [20].

3.3 ZnS nanoparticles as photocatalyst:

Environmental problems associated with organic pollutants and toxic water pollutants provide the impetus for sustained fundamental and applied research in the area of environmental remediation. Semiconductor photocatalysis offers the potential for complete elimination of toxic chemicals through its efficiency and potentially broad applicability. Various new compounds and materials for photocatalysis have been synthesized in the past few decades. A successful example

is TiO_2, a metal oxide often used as a catalyst in photochemistry, electrochemistry, environmental protection, and in the battery industry. Recently, transition metal sulphides, in particular ZnS and CdS have been intensively studied because of their unique catalytic functions compared to those of TiO_2. These studies have revealed that ZnS nanocrystals (NCs) are good photocatalysts as a result of the rapid generation of electron-hole pairs by photoexcitation and the highly negative reduction potentials of excited electrons. The photocatalytic properties occur not only in the photoreductive production of H_2 from water and photoreduction of CO_2, but also in the phototransformation of various organic substrates such as the oxidative formation of carbon-carbon bonds from organic electron donors, cis –trans photoisomerization of alkenes, and the photoreduction of aldehydes and their derivatives. The notable finding in nanometalized ZnS photocatalysis is an irreversible 2-electron-transfer photoreduction of organic substrates. A favourable shift of optical response into the visible region occurs subsequent to the doping of transition metal or rare earth metal ions, such as Ni^{2+} and Cu^{2+}. Therefore, ZnS NCs can also be used as effective catalysts for photocatalytic evolution of H_2 and photoreduction of toxic ions under visible light irradiation. An important application of ZnS is as a photocatalyst in environmental protection through the removal of organic pollutants and toxic water pollutants. ZnS nanomaterials have been used for the photocatalytic degradation of organic pollutants such as dyes, p-nitrophenol, and halogenated benzene derivatives in wastewater treatment. However, the applications of ZnS NCs in photocatalysis are limited to a considerable degree because of the high cost of their large scale production, coupled with the tremendous difficulties in separation, recovery, and recycling in industrial applications. Nevertheless, the studies have demonstrated that nanoporous materials with high surface to volume ratios can be successfully used in various catalysis, environmental engineering and sensor systems. Therefore the development of cost effective methods suitable for the large scale synthesis of ZnS nonporous nanostructures with high catalytic activity and easy separation represents a critical challenge to their practical applications [21].

3.4 Literature review:

Jin-Song Hu et al. [21] synthesized ZnS nanoparticles by chemical precipitation route. ZnS nanoparticles(ZnS NP's) were produced by a precursor thermolysis route in the presence of ethylene glycol as the reaction medium. In a typical experiment, zinc acetate (6mmol) and

thiourea(12mmol)were dissolved in ethylene glycol (150mL). PVP (4.8g) was then added to the solution with stirring and, after its complete dissolution, the clear solution was heated to 150^0C. After about 10 min. the solution turned milky white which indicated the initial formation of ZnS nanocrystals (ZnS NC's). The mixture was maintained at 145-155^0C for 3 hrs. and the color of reaction solution became milky white mixed with white yellow. The ZnS NP's obtained were separated from the reaction mixture by centrifugation, and washed several times with ultrapure water and ethanol to remove the impurities and PVP. Finally, the ZnS nonporous nanoparticles (NPNP's) were dried in a vacuum oven for 6 hrs. prior to being characterized. ZnS nanocrystallites were prepared in an argon atmosphere by mixing equal amounts of aqueous 0.05M solutions of $ZnSO_4$ and Na_2S in an ice bath with stirring. TEM images showed that the so-prepared ZnS NC's had a diameter ranging from 3 to 5 nm, and easily aggregated. A cylindrical pyrex flask was used as the photoreactor vessel. The reaction system containing eosin-B ($5*10^{-5}$M), sigma Aldrich chemical (30ml) and ZnS NPNP's catalyst (10mg) was magnetically stirred in the dark for 15 min. to reach the adsorption equilibrium of eosin B with the catalyst, and then exposed to light from a high pressure Hg lamp (125W). Commercial TiO_2 (Degussa P25) was adopted as the reference with which to compare the photocatalytic activity under the same experimental conditions. UV-Vis absorption spectra were recorded at different intervals to monitor the reaction. Degussa P25 and ZnS nonporous nanoparticles, under identical conditions were exposed to uv light. The ZnS NPNP photocatalyst showed much greater activity than that of Degussa P25.The degradation of eosin B in ZnS NPNPs followed first order kinetics. Exposure of the solution of eosin B to uv light for about 40 minutes resulted in complete decolorization. This difference in photocatalytic activity between ZnS NPNPs and Degussa P25 can be explained by the larger specific surface area of the former (ca.156.1 m^2gm^{-1} versus Degussa P25 powder ca.45 m^2gm^{-1}), and hence the stronger absorption of the ZnS NPNPs to the molecules of eosin B.

Ji Wook Jang et al. [22] synthesized nanosized N-doped ZnS with wurtzite phase by using organic-inorganic interaction in a solution at the mild temperature of 150^0C. By employing piperazine as an organic source, the metastable ZnS $(piperazine)_{0.5}$ nanohybrid materials formed in the initial stages of synthesis. Interlayer piperazine molecules connecting inorganic ZnS layers were moved out of the layered structure with the progress of synthetic reaction, and wurtzite ZnS

nanoparticles with trace nitrogen atoms were finally produced. Nitrogen atoms in piperazine were doped in ZnS in the phase transition. The organic piperazine molecules played two significant roles in the synthesis. The nucleophilic agent and the suppressant to inhibit the growth of particles. The N-doped ZnS had the decreased band-gap compared to pure ZnS. Change in band structure by N-doping can extend the application of ZnS upto a visible light regime. Both Z-24 and Z-24-400 exhibit considerable activities. The dye was almost degraded on Z-24-400 catalyst after 4.2 hrs. They also investigated the wavelength-dependance on the photocatalytic decomposition of organic dye. The catalyst decomposes 99.5% of the dye with the filter of λ >299.400 and 499 nm, they measured the whole photocatalytic activity over Z-24-400 catalyst and calculated the activity at the particular section of wavelengths. The catalyst decomposed 99.5% of the dye with the filter of λ>299 after irradiation of 1.5 hrs.

Jyoti P.Borah and her co-workers [20] reported on the growth of ZnS semiconductor nanocrystals embedded in a polymeric matrix(Polyvinyl alcohol) synthesized by a chemical route.The as obtained films were characterized by X-ray diffraction (XRD), transmission electron microscopy (TEM), UV-Vis absorption, and photoluminescence (PL) spectra. X-ray diffraction (XRD) study confirmed the formation of cubic phase of ZnS nanocrystals into the polymer matrix. The particle size variations were achieved by varying the pH in the starting solution. Transmission electron microscope image as well as XRD studies confirmed the nanometer size particle formation within the polymer matrix. The average particle size was found to lie in the range of 5-7 nm. A UV-Vis optical spectroscopy was carried out to determine the band-gap of the nanocrystalline ZnS thin film and it showed a blue shift with respect to the bulk value. The room temperature photoluminescence spectra of the films showed two peaks centered around 315 nm and 425 nm. They assigned the first peak due to band-gap transitions while the latter was due to sulfur vacancy in the films.

Hamid Reza Pouretedal and his co-workers [23] synthesized nanoparticles of zinc sulfide as undoped and doped with manganese, nickel and copper. They were used as photocatalyst in the photodegradation of methylene blue and safranin as color pollutants. Photoreactivity of doped zinc sulfide was varied with dopant, mole fraction of dopant to zinc ion, pH of solution, dosage of photocatalyst and concentration of dye. The characterization of nanoparticles was studied

using X-ray powder diffraction (XRD) patterns and UV–VIS spectra. The maximum degradation efficiency was obtained in the presence of $Zn_{0.98}Mn_{0.02}S$, $Zn_{0.94}Ni_{0.06}S$ and $Zn_{0.90}Cu_{0.10}S$ as nanophotocatalyst. The effect of dosage of photocatalyst was studied in the range of 20–250 mg/L. It was seen that 150.0 mg/L of photocatacyst is an optimum value for the dosage of photocatalyst. The most degradation efficiency was obtained in alkaline pH of 11.0 with study of photodegradation in pH amplitude of 2–12. The degradation efficiency was decreased in dye concentrations above of 5.0 mg/L for methylene blue and safranin dyes. In the best conditions, the degradation efficiency was obtained 87.3–95.6 and 85.4–93.2 for methylene blue and safranin.

Shiding Miao et al. [24] synthesized nanocomposites of zinc sulfide (ZnS) and montmorillonite (MMT) via a hydrothermal route. In this method, the MMT treated with hexadecyltrimethyl ammonium bromide (HTAB) aqueous solution was dispersed in the aqueous solution of thiourea and $Zn(OOCHCH_3)_2 \cdot 2H_2O$, and heated at 170 °C for about 4 h, resulting in ZnS-MMT composites. The as-prepared nanocomposites were characterized with X-ray diffraction, scanning electron microscopy, transmission electron microscopy, and nitrogen sorption analysis. It was demonstrated that the interlayer space of MMT was enlarged from 0.98 to 3.77 nm after the treatment with HTAB aqueous solution, and the ZnS nanoparticles were deposited on the layers of MMT. Nitrogen sorption analysis demonstrated that the specific surface area of the samples decreased from 39.2 m^2/g of the pristine MMT to 5.9 m^2/g of the final ZnS-MMT composites. The resulting ZnS-MMT nanocomposites (50.0 mg) could degrade eosin B completely in aqueous solution (75 ml, 3.2×10^{-5} M) within 20 min under UV irradiation.

Junping Li et al. [25] prepared hydrophilic ZnS nanocrystals with narrow size distribution via homogeneous precipitation using EDTA as stabilizer. The as-synthesized products were characterized with XRD, TEM, HRTEM and UV-Vis spectrum. UV-Vis spectra showed that ZnS nanocrystals exhibited strong quantum-confined effect with a blue shift in the band gap of light absorbance. The photocatalytic activity of these nanocrystals was also investigated for the liquid phase photocatalytic degradation of Basic Violet 5BN (BV5) dye under UV irradiation. It was found that the ZnS nanocrystals had good catalytic activity for photodegradation of BV5.

S. Wageh et al. [26] have synthesized ZnS quantum dots using mercaptoacetic acid as a stabilizer. The formation of samples occured as a result of a thermodynamically controlled cluster growth. A new absorption band was observed for samples refluxed at short times. The absorption band lied below the absorption edge of the particles, and it was attributed to vacancies and interstitial ions. The luminescence spectra showed some new characteristics. With a short refluxing time the concentration of point defects was high and they acted as traps for photoexcited carriers and as centers for radiative recombination. On the other hand with increasing refluxing time, the concentration of point defects decreased, which enhanced the luminescence associated with band edge recombination.

Yonghong Ni et al. [27] synthesized the ZnS (en) 0.5 complex with a cuboid morphology by a simple solvothermal method. SEM observations showed that the cuboids were formed due to the breaking of the lamellar products. By annealing in a vacuum and in air, ZnS (en) 0.5 could be converted into the wurtzite ZnS and ZnO. The research from the photocatalytic degradation of safranin T showed that ZnS was the strongest photocatalyst than ZnO and ZnS(en)0.5, the weakest. Moreover, ZnS(en) 0.5, ZnS, and ZnO could promote the electron transfers between Hb or catechol and the Au electrode. However, the abilities to accelerate the electron transfer of various modified electrodes were different in different systems. The ability in the system containing Hb was observed as ZnS > ZnO > ZnS (en) 0.5, which should be attributed to the change of the spatial surface. In the system including catechol, ZnS (en) 0.5 had a stronger ability to accelerate the electron transfer, which should be related to the presence of en molecules.

P.Yang and his co-workers [28] synthesized doped ZnS nanoparticles by precipitation from homogeneous solutions of zinc, copper, manganese and cadmium salt compounds, with S^{2-} as precipitating anion, formed by decomposition of thioacetamide. The fluorescence spectra of Cd^{2+} doped samples showed a red shift in emission (wavelength range from 450 nm to 620 nm) and excitation wavelengths. A relatively broad emission (color range from blue to yellow) was observed. The fluorescence spectra of samples co-doped with Cu^{2+} and Mn^{2+} showed very strong visible-light emission from co-doped ZnS nanocrystals at room temperature. The emission band of ZnS nanoparticles was observed at 450 nm. Cu^{2+} doped ZnS nanocrystals had two emission bands. One was observed at 450 nm while the other at 530 nm. The emission band of ZnS

nanoparticles co-doped with Cu^{2+} and Mn^{2+} was at 520–540 nm and their fluorescence intensity was dramatically enhanced as compared to that of Cu^{2+} doped and Mn^{2+} doped ZnS nanocrystals. Two kinds of transition metal-activated ZnS nanoparticles formed a new class of luminescent materials with strong and stable visible light emission.

Ali Azam Khosravi and his co-workers [29] prepared free-standing powder of zinc sulphide quantum particles using a chemical route. X-ray diffraction analysis showed that the diameter of the particles was 21±2 Å which was smaller than the Bohr exciton diameter for zinc sulphide. UV absorption showed an excitonic peak centered at 300 nm corresponding to an energy gap of 4.1±0.1 eV. These particles showed a luminescence band at 424 nm. The quantum particles could be doped with copper during synthesis without altering the UV absorption or x-ray diffraction pattern. However, doping shifted the luminescence to 480 nm, green wavelength in the visible region.

Franco et al. [30] synthesized distinct nanocrystalline TiO_2 capped ZnS samples using a chemical deposition method. The materials characterization showed that the presence of ZnS onto TiO_2 surface results in a red shift of the material band edge when compared with the initial semiconductor. The photocatalytic activity of the prepared nanocomposites was tested on the decolorization of methylene blue (MB) aqueous solutions. The dye photodecolorization process was studied considering the influence of experimental parameters such as catalyst concentration, TiO_2/ZnS ratio, pH and methylene blue adsorption rate. The material with the best catalytic activity towards the methylene blue photodecolorization was the TiO_2 doped with 0.2% of ZnS. The complete photodecolorization of a 20 ppm methylene blue solution, at natural pH was achieved in less than 20 min, nearly 70 min faster than the TiO_2 photoassisted process.

W.Q. Peng et al. [31] investigated the room-temperature photoluminescence (PL) of copper doped zinc sulfide (ZnS:Cu) nanoparticles. These ZnS:Cu nanoparticles were synthesized by a facile wet chemical method, with the copper concentration varying from 0 to 2 mol%. By Gaussian fitting, the PL spectrum of the undoped ZnS nanoparticles was deconvoluted into two blue luminescence peaks (centered at 411 nm and 455 nm, respectively), which both can be attributed to the recombination of the defect sates of ZnS. But for the doped samples, a third peak at about 500 nm was also identified. This green luminescence originates from the

recombination between the shallow donor level (sulfur vacancy) and the t_2 level of Cu^{2+}. With the increase of the Cu^{2+} concentration, the green emission peak is systematically shifted to longer wavelength. In addition, it was found that the overall photoluminescence intensity is decreased at the Cu^{2+} concentration of 2%. The concentration quenching of the luminescence may be caused by the formation of CuS compound. Synthesis and photoluminescent properties of ZnS nanocrystals doped with copper and halogen.

Manoj Sharma et al. [32] studied the energy transfer mechanism from different capping agents to intrinsic luminescent vacancy centres of ZnS nanoparticles. Nanoparticles of capped and uncapped ZnS were prepared by co-precipitation reaction. These nanoparticles were sterically stabilized using organic polymers – polyvinylpyrrolydone, 2-mercaptoethanol, and thioglycerol. Monodispersed nanoparticles were observed under TEM for both capped and uncapped ZnS nanopowders. However, for uncapped ZnS nanopowders, tendency for formation of nanorod like structure exist. Size of ZnS crystallites was calculated from X-ray diffraction pattern. The primary crystallite size estimated from X-ray diffraction pattern was found to be 1.95–2.20 nm for capped nanostructures and 2.2 nm for uncapped nanostructures. FTIR spectra were conducted to confirm capping. Zeta potential measurements were done to check the stability of dispersed nanoparticles. Band gap measurement was done by UV–visible spectrophotometer. Excitation and emission spectra were also performed in order to compare optical properties in various samples. Increase in emission intensity and band gap was observed by adding different capping agents in comparison to uncapped ZnS nanoparticles. The results showed that in capped ZnS nanoparticles the mechanism of energy transfer from capping layer to photoluminescent vacancy centres was more pronounced.

Manoj Sharma and his co-workers [33] synthesized luminescent nanoparticles of zinc sulphide (ZnS) with and without capping agent. Nanoparticles of ZnS are prepared by a coprecipitation reaction. Based on Ostwald ripening and surface passivation, they have discussed a mechanism for the formation of ZnS nanoparticles. The reaction proceeded with the nucleation of ZnS crystals, which were immediately passivated by the anions in the solution. This in turn attracted cations including Zinc and which contributed to the growth of the crystal. The nanoparticles were sterically stabilized using organic polymer Poly Vinyl Pyyrodine (PVP). The change in optical and morphological properties of ZnS nanoparticles was observed by using organic

capping agent. The nanoparticles were of 6–8 nm in diameter as from TEM, each containing primary crystallites of size 2.2 nm that were estimated from the X-ray diffraction patterns. Band gap measurements done by UVvisible spectrophotometer and excitation spectra showed that band gap increased by introducing capping material. Photoluminescence studies showed that emission intensity increased for capped sample.

Manoj Sharma et al. [34] have synthesized ZnS:Mn^{2+} doped semiconductor using chitosan as capping agent. They have reported deliberate color modulation for chitosan capped ZnS:Mn^{2+} nanoparticles (NPs) synthesized in single step instead of many samples of different size. The tunable behavior was achieved by varying the excitation wavelength in same sample. Shifting of emission peak from dopant related emission at 590 nm to 481 nm defect related emission (Sulfur vacancy to Zn^{2+}) and 421 nm (sulfur vacancy to valence band) has been observed. The work illustrated coupling between Frenkel exciton in organic polymers with Wannier exciton in inorganic semiconductors which has been observed for the present nanophosphors. Synthesized chitosan capped ZnS: Mn^{2+} NPs were characterized by x-ray diffraction, high-resolution transmission electron microscopy, energy dispersive x-ray, and Fourier transform infrared for structural studies. UV visible absorption spectroscopy and Photoluminescence studies were done to observe optical behavior. Biocompatibility of chitosan functionalized ZnS:Mn quantum dots was also verified with bacteria (staphylococcus aureus).

CHAPTER – 4

Experimental

Chemical precipitation:

A reaction that occurs when aqueous solutions of anions (negatively charged ions) and cations (positively charged ions) combine to form a compound that is insoluble, meaning it does not dissolve in water is called chemical precipitation. The insoluble solid is called the precipitate, and the remaining liquid is called the supernate. Precipitation reactions occur when a cation and an anion of two aqueous solutions react to form an ionic, insoluble solid, known as a precipitate in the solution where the reaction is taking place. However, based on the solubility rules not all aqueous reactions form precipitates. Therefore, one must first consult the solubility rules before they can determine if a precipitate will form and make a net ionic equation.

Properties of Precipitates: Precipitates are the products of a precipitation reaction, in which certain cations and anions combine to produce and insoluble solid. The determining factors of the formation of a precipitate can vary: some depend on temperature, such as solutions used for buffers, while others are dependent only on solution concentration. The solids produced in precipitate reactions are crystalline. The solid can then be suspended throughout the liquid or it can fall to the bottom of the solution. The liquid that remains above the precipitate is called the supernatant liquid. Here is a diagram of the formation of a precipitates in the solution.

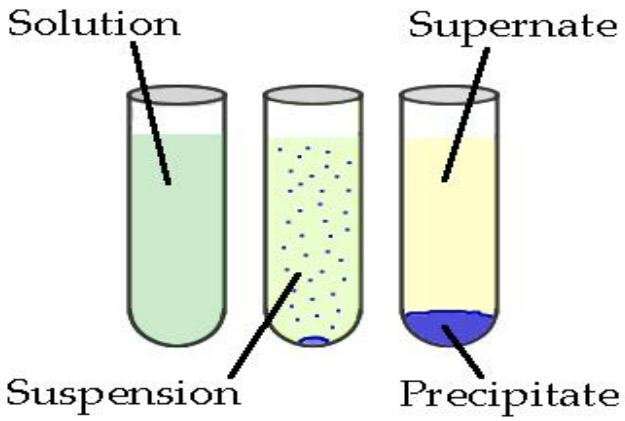

Fig. 4.1 - Chemical precipitation

Zinc sulphide (ZnS) nanoparticles were synthesized by chemical precipitation method [34-36] by adding appropriate amount of zinc acetate solution and S^{2-} as precipitating anion formed by decomposition of sodium sulphide (Na_2S). 0.5 M zinc acetate ($Zn(CH_3COO)_2.2H_2O$) was dissolved in distilled water and 0.5 M sodium sulfide (Na_2S) was dissolved in distilled water separately. These solutions were stirred for 15 minutes using magnetic stirrer for 15 minutes separately. As a capping agent, different concentrations of capping agents (sodiumpolyphosphate (SPP) 1%, SPP 2%, thioglycerol (TG) 1%, TG 2%, mercaptoethanol (ME) 1%, ME 2%, sodium hexametaphosphate (SHMP) 1%, SHMP 2%, sodiumtripolyphosphate (STPP) 1%, STPP 2%) were also dissolved in distilled water and stirred for 15 minutes using magnetic stirrer. Capping agents were used to control the particle size. To the stirred solution of zinc acetate, solution of capping agent was poured drop by drop. After 15 minutes, solution of sodium sulphide was poured drop by drop. The precipitate appears soon after the addition of sodium sulphide, indicating the flocculation phenomenon occurring in the system. After that stirring was done overnight. The precipitated particles were filtered using whatman 40 filter paper and were centrifuged at 4000 rpm. To remove the last traces of adhered impurities, the particles were washed several times using distilled water and acetone. The washed particles were dried in an oven at 60ºC. The ZnS nanoparticles were characterized by X-ray diffraction (XRD) using Panalytical's X'Pert Pro with Cu Kα radiation. Optical absorbance of ZnS particles were recorded with an UV-Visible spectrophotometer with a scan speed of 200 nm / min in the range of 190–600 nm. For the measurement of UV-VIS absorbance, a small amount of the dried particles were dispersed in distilled water by sonication process.

CHAPTER - 5

Results and discussion

5.1 XRD analysis:

For the XRD analysis, fine powder samples of ZnS nanoparticles capped with different concentrations of sodiumtripolyphosphate(STTP)1%, STTP 2%, sodiumpolyphosphate(SPP)1%, SPP 2% were mounted on the sample holder ensuring that the powder consist of randomly oriented crystallites. The capped ZnS nanoparticles were characterized by X-ray diffraction (XRD) using Rigaku (model D–maxIIIC) diffractometer with Cu Kα radiation. Crystallite size of ZnS nanoparticles were calculated by following Scherrer's equation

$$t = k \lambda / \beta \cos\theta$$

where k = 0.9, t, the crystallite size (Å), λ(Å), the wavelength of Cu Kα radiation and β, the corrected half width of the diffraction peak. In case of fine particles, with reduction in the size of the particles, the XRD lines get broadened, which indicates clearly that particle size has been reduced. From Fig. 6.1(a), (b), (c), (d), it is observed that XRD patterns were very broad with three peaks corresponding to the (111), (220) and (311) planes. The average crystallite size calculated using the Scherer's formula is 2-3 nm.

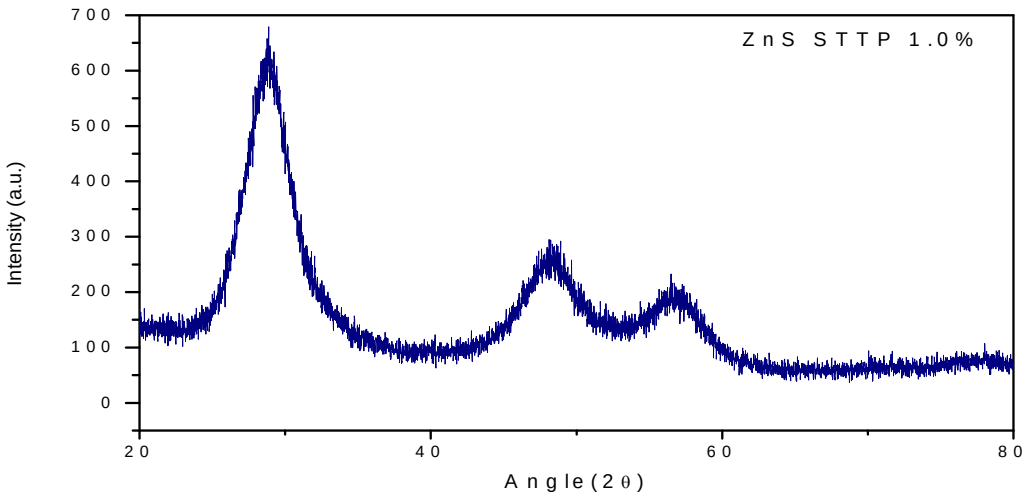

Fig. 5.1(a) – XRD of ZnS nanoparticles capped with STTP 1.0%

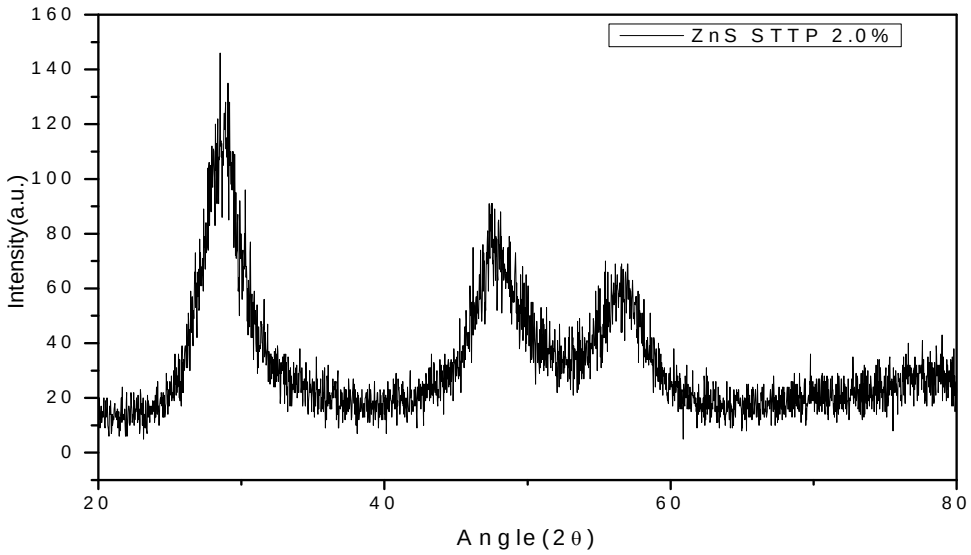

Fig. 5.1(b) – XRD of STTP 2% capped ZnS nanoparticles

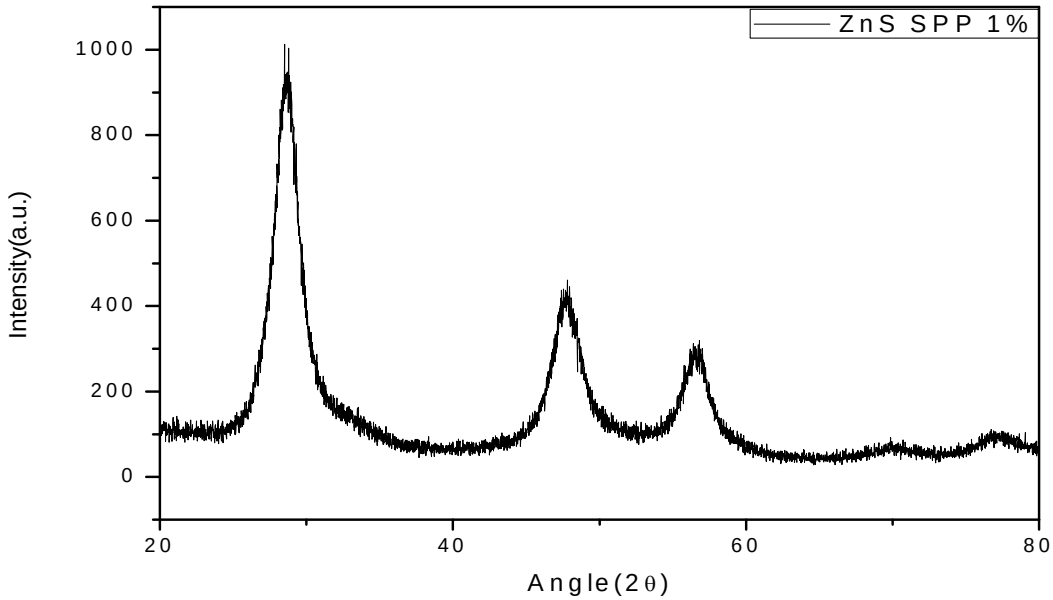

Fig. 5.1(c) – XRD of ZnS nanoparticles capped with SPP 1%

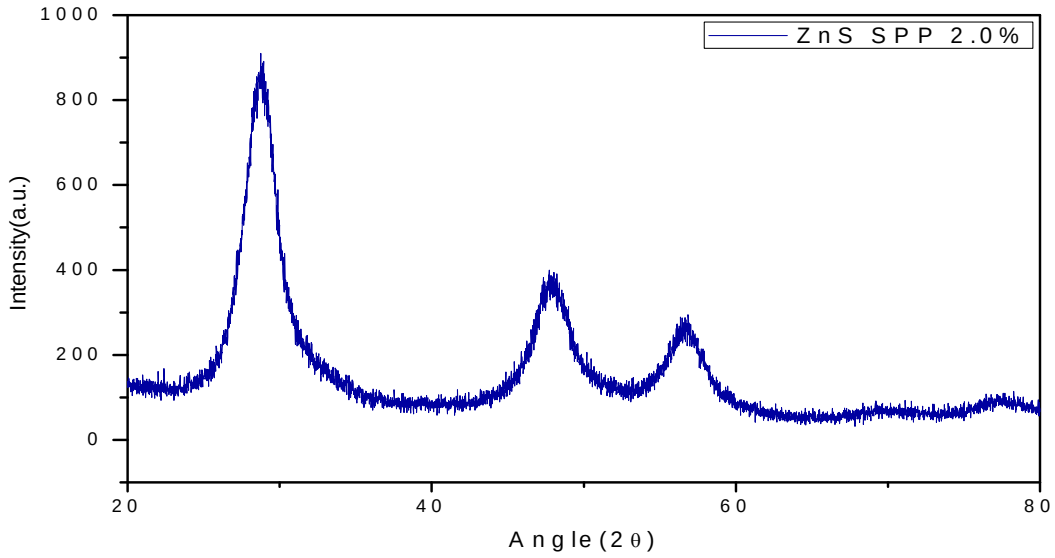

Fig. 5.1(d) – XRD of ZnS nanoparticles capped with SPP 2.0%

Three peaks have been observed in the span ranging from 5º to 100º. These peaks correspond to FCC structure. It is to be noted that, the peaks observed in the XRD patterns match well with those of the β-ZnS (cubic) reported in the JCPDS Powder Diffraction. Intensities of the three most important peaks of ZnS, namely <111>, <220> and <311> reflections corresponding to 28.5º, 47.6º and 56.4º respectively do not deviate from the Powder Diffraction File intensities. Broadening of the XRD peaks indicates the formation of ZnS nanocrystals. Elongation of the XRD pattern in case of capped nanoparticles also shows the surface passivation.

5.2 Scanning Electron Microscopy:

From Fig. 5.2(a), it is clear that ZnS nanoparticles exhibit significant confinement effects.

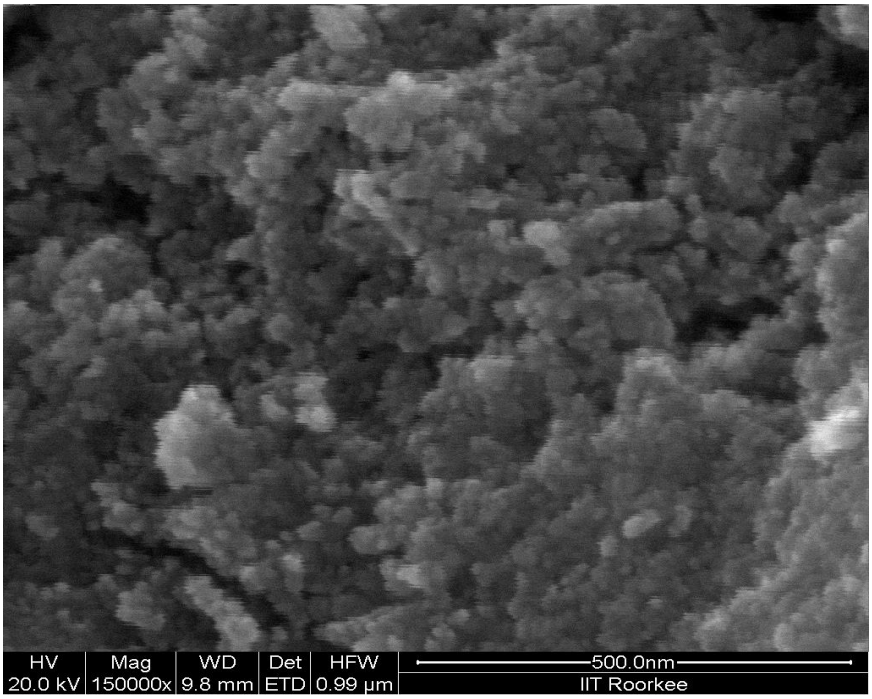

Fig. 5.2(a) – SEM image of TG capped ZnS nanoparticles

5.3 Energy Dispersive X-Ray Analysis (EDAX):

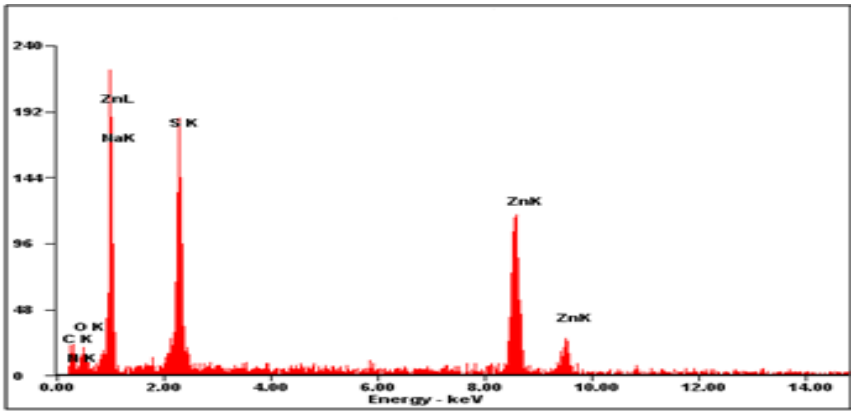

Fig.5.3 – EDX graph of TG capped ZnS nanoparticles

The corresponding EDAX spectrum is shown in Fig. 5.3 which shows presence of zinc and sulphur ions in larger amounts along with some carbon and oxygen in less amount which can be assigned to surface adsorbed polymer thioglycerol.

5.4 UV-VIS spectrophotometer results:

Optical study of capped ZnS nanoparticles is done using uv-vis spectrophotometer. For the measurement of UV-VIS absorbance, a small amount of the dried particles were dispersed in distilled water by sonication process. Optical absorbance of the ZnS particles were recorded with an UV-Visible spectrophotometer (Model: Specord-Germany) with a scan speed of 200 nm/min in the range 190–600 nm. The graphs below show the absorption spectra of ZnS nanoparticles with different concentrations of different capping agents.

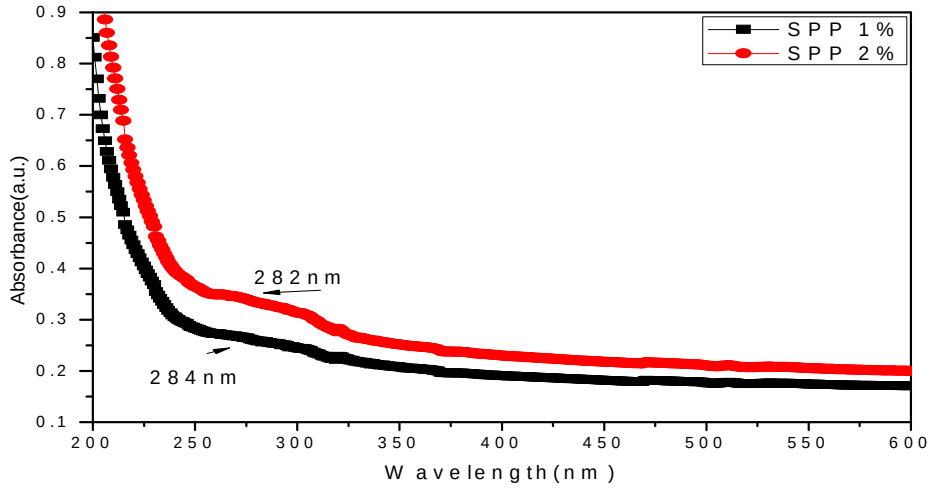

Fig. 5.4(a) – UV-VIS absorption spectra of ZnS nanoparticles capped with SPP 1% and SPP 2%

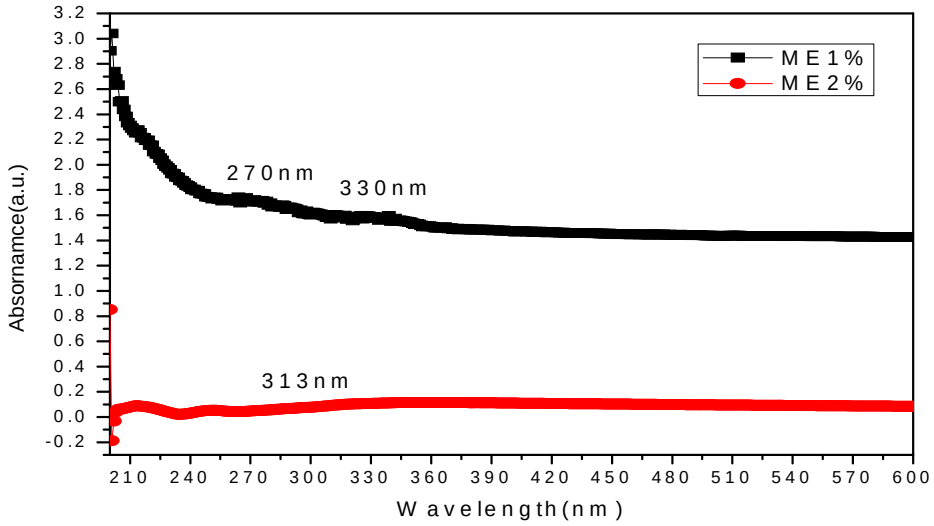

Fig. 5.4(b) – UV-VIS absorption spectra of ZnS nanoparticles capped with ME 1% and ME 2%

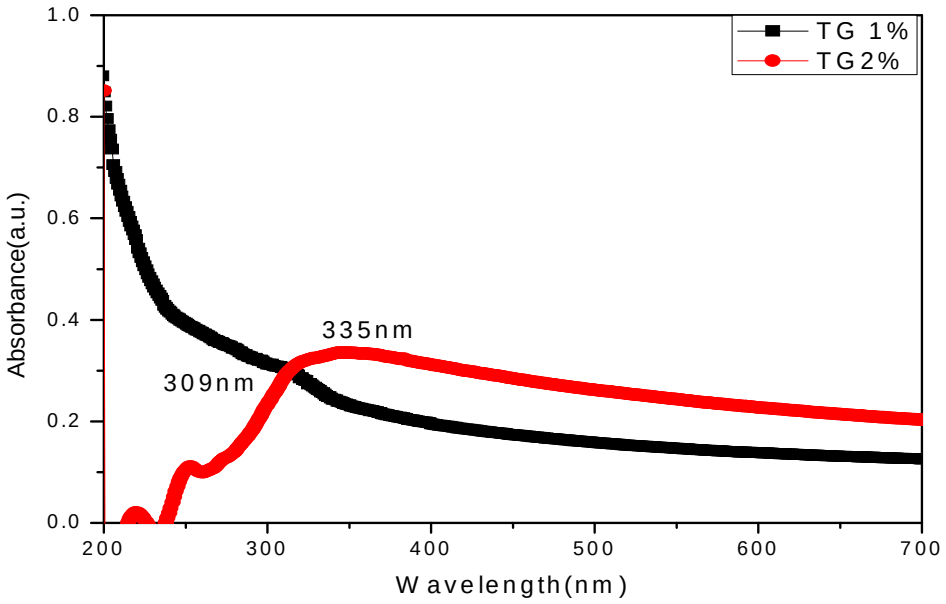

Fig. 5.4(c) – UV-VIS spectra of ZnS nanoparticles capped with TG 1% and TG 2%

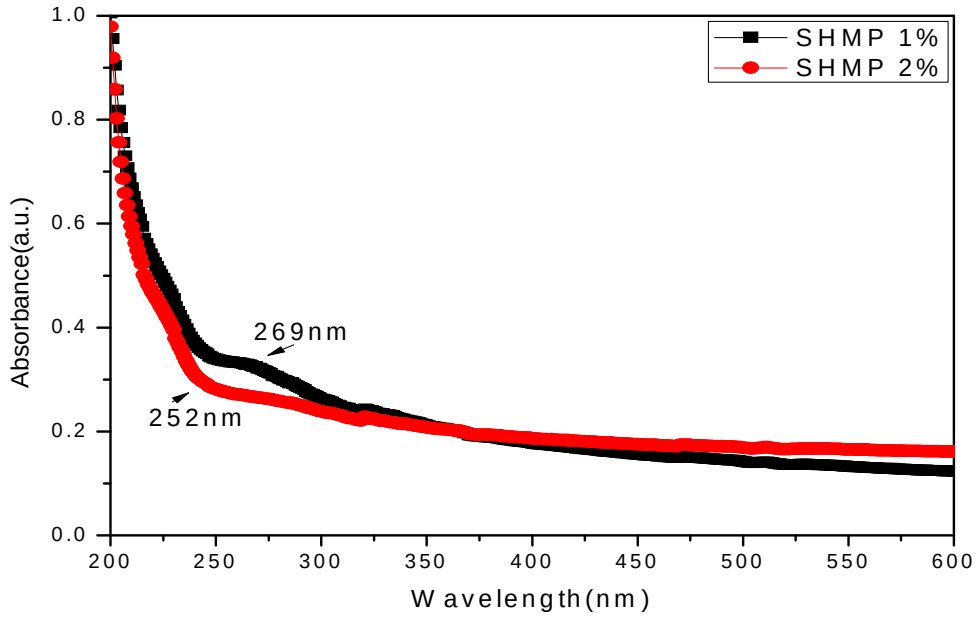

Fig. 5.4(d) – UV-VIS spectra of ZnS nanoparticles capped with SHMP 1% and SHMP 2%

From Fig. 5.4(a), the absorption edge for SPP 1% capped ZnS nanoparticles is observed at 284 nm and the corresponding band-gap comes out to be 4.3 eV. Similarly the observed absorption edge in case of SPP 2% capped ZnS nanoparticles comes out to be 282 nm and corresponding band-gap is 4.4 eV. Similarly the values of absorption edges and the corresponding band-gaps for different concentrations of capping agents is given in table 5.1. The blue shift of absorption edge compared to bulk ZnS (onset is at 340 nm) is because of quantum confinement effect of ZnS nanoparticles. From these calculated values, we observe blue shift in absorption spectra of capped ZnS nanoparticles and increase in energy band-gap as compared to that of bulk ZnS.

Table 5.1 – Different concentrations of capping agents, their absorption edges and corresponding band-gaps

Capping agent	Absorption edge (nm)	Band-gap (eV)
SPP 1%	284	4.3
SPP 2%	282	4.4
TG 1%	309	4.0
TG 2%	325	3.7
ME 1%	330	3.7
ME 2%	313	3.9
SHMP 1%	269	4.6
SHMP 2%	252	4.9

The absorption edges of the nanocrystallites are also sharp, indicating that the synthesized particles have relatively narrow size distributions. As the bulk band-gap of ZnS is 3.6 eV, it means there is a strong quantum confinement in case of capped ZnS quantum dots in our case.

5.5 Photoluminescence studies:

Fig. 5.5(a) shows PL emission spectra of SHMP (1%, 2%) capped ZnS nanoparticles at 325 nm excitation. It shows emission peak at 446 nm and 366 nm for SHMP 1% and SHMP 2%

respectively. Similarly fig. 5.5(b), 5.5(c), 5.5(d) shows PL spectra corresponding to excitation wavelength of 325 nm for different concentrations of capping agents (SPP, TG, ME).

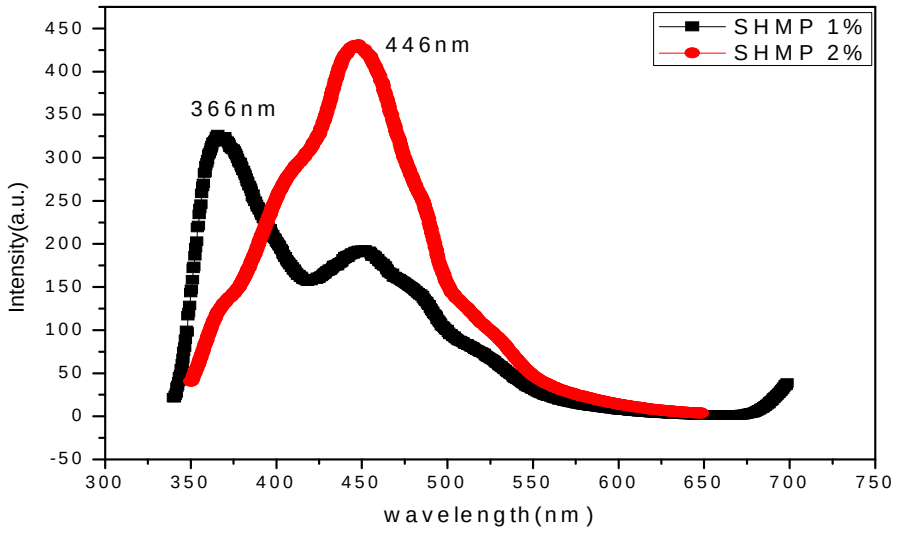

Fig. 5.5(a) – PL emmission spectra of ZnS nanoparticles capped with SHMP 1% and SHMP 2%

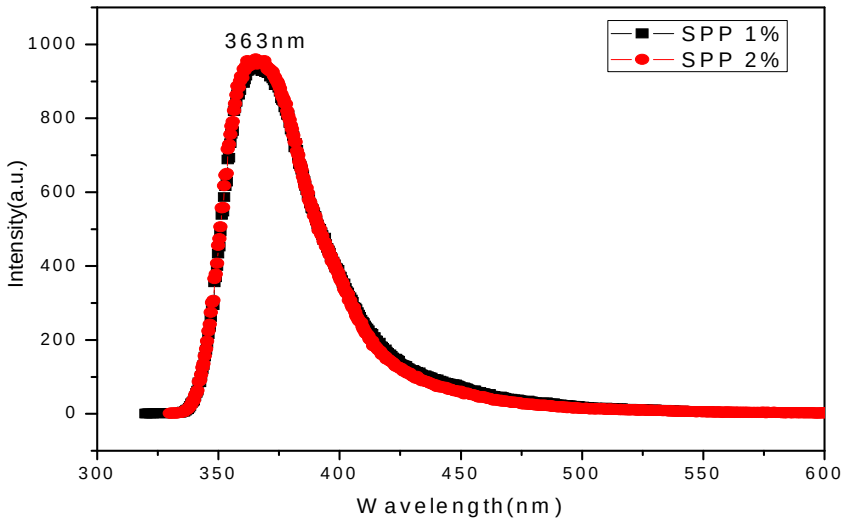

Fig. 5.5(b) – PL emmission spectra of ZnS nanoparticles capped with SPP 1% and SPP 2%

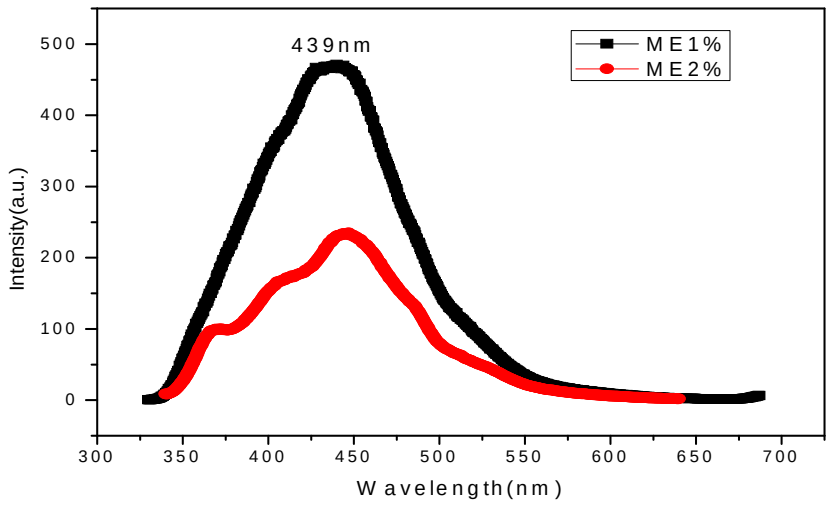

Fig. 5.5(c) – PL emmission spectra of ZnS nanoparticles capped with ME 1% and ME 2%

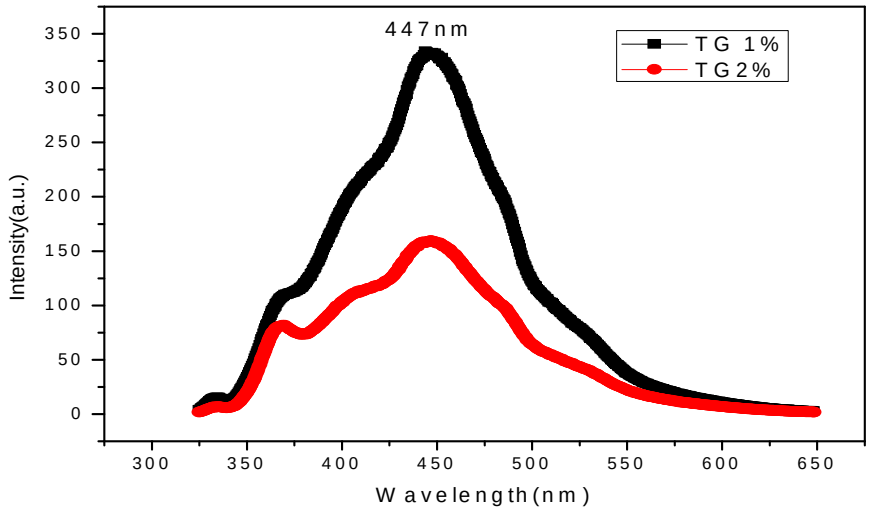

Fig. 5.5(d) – PL emmission spectra of ZnS nanoparticles capped with TG 1% and TG 2%

Table 5.2 – Excitation and emission wavelengths of capped ZnS nanoparticles

Capping agents	Excitation wavelength(nm)	Emission wavelength(nm)
SHMP 1%	325	366
SHMP 2%	325	446
SPP 1%	325	363
SPP 2%	325	363
ME 1%	325	439
ME 2%	325	447
TG 1%	325	447
TG 2%	325	445

There are two emission peaks around 363 nm and 445 nm in all samples. Emission peak at 363 nm is due to transfer of energy from sulphur vacancies to valence band and 445 nm emission is due to transfer of energy from sulphur vacancies to zinc vacancies which are lying in the band-gap of host ZnS. This shows synthesized nanoparticles exhibit two possible colours in violet and blue region which is achieved by using different capping agents and by changing their concentration (1%, 2%). Further, there is change in PL peak intensity in some samples by changing capping agent concentrations as shown in fig. 5.5 (a-d). Then decrease in intensity by increase in capping concentration in some samples is explained by the fact that after specified concentration of capping agents, further increase in their concentration, increases the existence of defect states in samples and further decreases its PL intensity.

5.6 Photocatalytic degradation of dye using ZnS nanoparticles:

Degradation of dye was done using TG 1% capped ZnS nanoparticles. Absorbance spectra is shown in the fig. 5.6. When nanoparticles were not added to the bromophenol blue dye, UV-VIS

spectra showed the absorbance peak at 550 nm. After that a known amount of capped ZnS nanoparticles was added to 50 ppm of dye and was placed in uv reactor. UV light is being absorbed by NPs since their absorbance lies in this range as shown above in UV – Vis analysis. So, ZnS NPs transfer energy to dye molecules which further degrade it. Uv-vis spectra of dye + ZnS nanoparticles was taken after an interval of 30 min. It showed the decrease in absorbance (fig. 5.6). The decrease in absorbance indicates the degradation of dye. After 30 min. spectra was again taken and further decrease in absorbance was observed. This procedure was done 6 times. After 3.5 hours, absorbance was decreased sufficiently which indicates the complete degradation of dye.

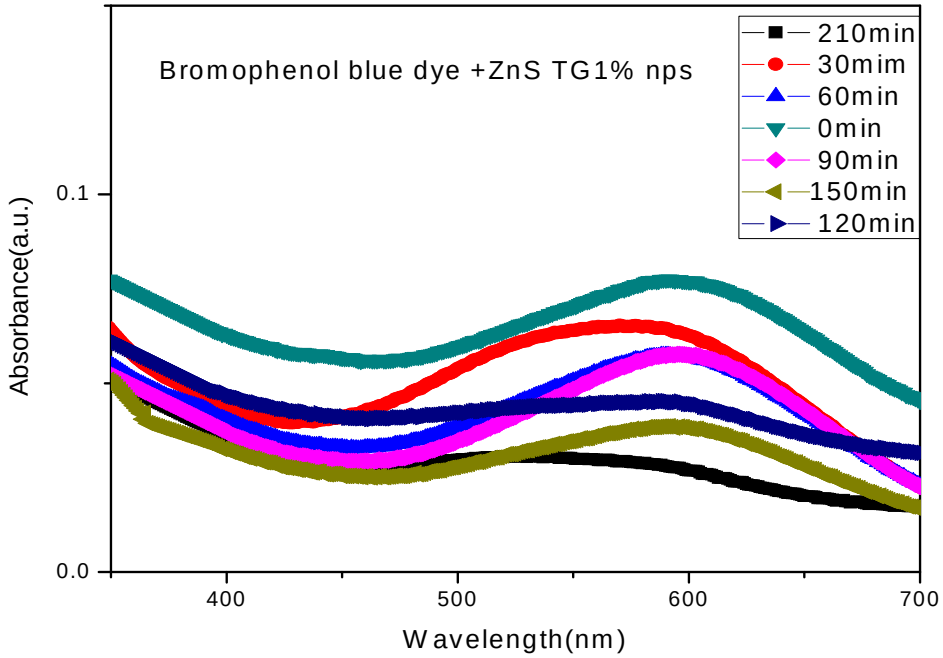

Fig. 5.6 – UV-VIS spectra of bromophenol blue dye + ZnS TG 1% nanoparticles

CHAPTER – 6

Conclusions

Monodispersed ZnS nanoparticles have been synthesized via chemical precipitation method with average size of 2-8 nm with different concentrations of TG, ME, SPP, SHMP and STTP as capping agent and double distilled water as solvent. The nanostructures of the prepared ZnS nanoparticles have been confirmed using UV-VIS absorption, XRD, and SEM micrograph analysis. The absorption edge in uv-vis spectra also shows that the ZnS nanoparticles undergo blue shift. The PL emissions from the ZnS nanoparticles dispersed in water have been measured under 325 nm UV light excitations. The maximum PL emission has been observed covering the whole 360-445 nm visible region of the electromagnetic spectrum when 325 nm wavelengths are used for excitation. The strong violet and blue luminescence we observed, demonstrates the good quality of the prepared ZnS nanoparticles. As suggested and confirmed by others that such low energy emissions are assigned to the surface states. The density of surface states in the nanocrystals would increase with a decrease in the size of crystallites of the prepared nanocrystals, due to the increased surface-to-volume ratio having smaller crystallites. This would reduce the probability of excitonic emission via non-radiative surface recombination. With changed concentrations of capping agents, two emission peaks corresponding to defect states are observed. 50 ppm of Bromophenol dye was effectively treated using ZnS nanoparticles. The reduction in absorbance of dye suggests that the dye molecules were completely mineralized along with colour removal. It can be concluded that the ZnS assisted photocatalytic degradation of textile dyes may be a versatile, economic and environment friendly which is efficient method of treatment.

References

[1] Kahn, Jennifer, "Nanotechnology", *National Geographic* (2006) 98-119

[2] http://www.nanotech-now.com

[3] http://www.wikipedia.com

[4] http://www.nanosense.org

[5] http://www.worsleyschool.net

[6] http://www.tutorvista.com

[7] http://www.nanowerk.com

[8] http://www.gitam.edu

[9] http://www.tutorvista.com

[10] http://www.purdue.edu

[11] http://www.hk-phy.org

[12] http://www.files.chem.vt.edu

[13] Hao Zhang, Zhen Zhou and Bai Yang, **The influence of carboxyl groups on the photoluminescence of mercaptocarboxylic Acid-Stabilized CdTe nanoparticles**, *Journal of Physical Chemistry*, **107** (2003) 8-13

[14] Zorn, M. E. Tompkins, D. T. Zeltner, W. A. Anderson, M. A., **Catalytic and photocatalytic oxidation of ethylene on titania-based thin-films**, *Environ. sci. technol.* **34** (2000) 5206

[15] A. Fujishima and K. Honda, **Photocatalytic splitting of water on TiO_2 electrodes**, *Nature*, **238** (1972) 37

[16] B. Neppolian, S. Sakthivel, Banumathi Arabindoo, M. Palanichamy and V. Murugesan, **Kinetics of photocatalytic degradation of reactive yellow 17 dye in aqueous solution using uv irradiation**, *Journal of Environmental Science and Health*, **36** (2001) 203-213

[17] K. Byrappa, A. K. Subramani, S. Ananda, K. M. Lokanatha rai, R Dinesh and M. Yoshimura, **Photocatalytic degradation of rhodamine B dye using hydrothermally synthesized ZnO**, *Bull. Mater. Sci.*, **29** (2006) 433–438.

[18] D. Beydoun, R. Amal, G. Low and S. McEvoy, **Role of nanoparticles in photocatalysis**, *Journal of Nanoparticle Research*, **1** (1999) 439–458

[19] Howe R. F., **Recent developments in photocatalysis**, *Dev. Chem. Eng. Mineral Processes*, **6** (1998) 55-84

[20] Jyoti P. Borah, J. Barman, K.C.Sarma, **Structural and optical properties of ZnS nanoparticles**, *Chalcogenide Letters*, **5** (2008), 201-208

[21] Jin-Song Hu, Ling-Ling Ren, Yu-Guo Guo, Han-Pu Liang, An –Min Cao, Li-Jun Wan, and Chu-Li Bai, **Mass Production and High Photocatalytic Activity of ZnS Nanoporous Nanoparticles**, *Angew. Chem. Int. Ed.*, **44 (**2005) 1269 –1273

[22] Ji Wook Jang, Sun Hee Choi, Jum Suk Jang, Jae Sung Lee, Seungho Cho and Kun-Hong Lee, **N-Doped ZnS Nanoparticles Prepared through an Inorganic-Organic Hybrid Complex ZnS.(piperazine)0.5**, *J.Phys.Chem.*C, **113** (2009) 20445–20451

[23] Hamid Reza Pouretedal, Abbas Norozi, Mohammad Hossein Keshavarz and Abolfazl Semnani, **Nanoparticles of zinc sulfide doped with manganese, nickel and copper as nanophotocatalyst in the degradation of organic dyes**, *Journal of Hazardous Materials*, **162** (2008) 674-681

[24] Shiding Miao, Zhimin Li, Buxing Han, Haowen Yang, Zhenjiang Miao and Zhenyu Sun, **Synthesis and characterization of ZnS-montmorillonite nanocomposites and their**

application for degrading eosin B, *Journal of Colloid and Interface Science*, **301**, (2006) 116-122

[25] Junping Li, Yao Xu, Yong Liu, Dong Wu and Yuhan Sun, **Synthesis of hydrophilic ZnS nanocrystals and their application in photocatalytic degradation of dye pollutants**, *China Particuology*, **2** (2004) 266-269

[26] S.Wageh, Zhao Su Ling and Xu Xu-Rong, **Growth and optical properties of colloidal ZnS nanoparticles**, *Journal of Crystal Growth* **255** (2003) 332–337.

[27] Yonghong Ni, Xiaofeng Cao, Guangzhi Hu, Zhousheng Yang, Xianwen Wei, Yonghong Chen and Jun Xu, **Preparation, Conversion, and Comparison of the Photocatalytic and Electrochemical Properties of ZnS(en)0.5, ZnS, and ZnO**, *Crystal Growth and Design*, **7** (2007) 280-285

[28] P.Yang, M.Lu, D.Xu, D.Yuan and G.Zhou, **Synthesis and photoluminescence characteristics of doped ZnS nanoparticles**, *Appl. Phys. A*, **73** (2001) 455–458

[29] Ali Azam Khosravi, Manisha Kundu, Lalita Jatwa, and S. K. Deshpande, U. A. Bhagwat, Murali Sastry and S. K. Kulkarni, **Green luminescence from copper doped zinc sulphide quantum particles**, *Appl. Phys. Lett.*, **67** (1995) 18

[30] A. Franco, M.C. Neves, M. M. L. Ribeiro Carrott, M.H. Mendonça, M.I. Pereira and O.C. Monteiro, **Photocatalytic decolorization of methylene blue in the presence of TiO_2/ZnS nanocomposites**, *Journal of Hazardous Materials*, **161** (2009), 545-550

[31] W.Q. Peng, G.W. Cong, S.C. Qu and Z.G. Wang, **Synthesis and photoluminescence of ZnS:Cu nanoparticles,** *Optical Materials*, **29** (2006) 313–317

[32] Manoj Sharma, Sunil Kumar and O. P. Pandey, **Study of energy transfer from capping agents to intrinsic vacancies/defects in passivated ZnS nanoparticles**, *Journal of Nanoparticle Research*, (2010) DOI 10.1007/s11051-009-9844-2 (in press)

[33] Manoj Sharma, Sunil Kumar and O.P.Pandey, **Photo-physical and morphological studies of organically passivated core-shell zns nanoparticles**, *Digest Journal of Nanomaterials and Biostructures*, **3** (2008) 189 – 197

[34] Manoj Sharma, Sukhvir Singh and O. P. Pandey, **Excitation induced tunable emission in biocompatible chitosan capped ZnS nanophosphors,** *Journal of Applied Physics*, **107** (2000) 104319